

1 Preprint published at EarthArxiv:

2 <https://doi.org/10.31223/X54M0V>

3  
4  
5 Indian Plate paleogeography, subduction, and horizontal  
6 underthrusting below Tibet: paradoxes, controvercies,  
7 and opportunities

8  
9  
10 DOUWE J.J. VAN HINSBERGEN

11  
12  
13 Department of Earth Sciences, Utrecht University, Princetonlaan 8A, 3584 CB  
14 Utrecht, the Netherlands. [d.j.j.vanhinsbergen@uu.nl](mailto:d.j.j.vanhinsbergen@uu.nl)

15  
16  
17 *This is a non-peer reviewed preprint. This manuscript is submitted for publication in*  
18 *NATIONAL SCIENCE REVIEW. Subsequent version of this manuscript may differ*  
19 *slightly in content. Once accepted, the published version will be available through the*  
20 *'peer-reviewed publication doi' on this website. Feel free to contact me with comments.*

## 14 Keywords

15 Collision, orogenesis, subduction, reconstruction, Himalaya, Tibet

16

## 17 Abstract

18 The India-Asia collision zone is the archetype to calibrate geological responses of  
19 continent-continent collision, but hosts a paradox: there is no orogen-wide geological  
20 record of oceanic subduction after initial collision around 60-55 Ma, yet thousands of  
21 kilometers of post-collisional subduction occurred before arrival of unsubductable  
22 continental lithosphere that currently horizontally underlies Tibet. I show that  
23 kinematically restoring incipient horizontal underthrusting accurately predicts geologically  
24 estimated diachronous slab break-off, unlocking the Miocene of Himalaya-Tibet as natural  
25 laboratory for unsubductable lithosphere convergence. Additionally, three end-member  
26 paleogeographic scenarios exist with different predictions for the nature of post-collisional  
27 subducting lithosphere but each is defended and challenged based on similar data types.  
28 Here, I attempt at breaking through this impasse by identifying how the three  
29 paleogeographic scenario each challenge paradigms in geodynamics, orogenesis,  
30 magmatism, or paleogeographic reconstruction and identify opportunities for  
31 methodological advances in paleomagnetism, sediment provenance analysis, and  
32 seismology to conclusively constrain Greater Indian paleogeography.

33

## 34 Introduction

35 With major continents being too buoyant to subduct – the reason why they can  
36 become billions of years old (1) – colliding continents are associated with subduction  
37 arrest, plate reorganization, and orogenesis (2), seaway closure, mountain building, and  
38 atmospheric barrier formation (3), and exchange and diversification of terrestrial biota  
39 (4). The orogen at the India-Asia continental collision zone is the archetype to calibrate  
40 the relationships between collision, orogenic architecture, history, and dynamics,

41 resulting magmatism and mineralization, as well as climatic and biological responses (3,  
42 5-8). But long-standing paradoxes and controversies in tectonic history have led to an  
43 impasse, making using the full potential of the archetype difficult.

44 Geophysical imaging has revealed that Indian continental lithosphere has  
45 horizontally underthrust the Tibetan upper plate (9-14). This is consistent with the  
46 paradigm of unsubductability of thick continental lithosphere (2) and offers opportunities  
47 to study the dynamics of and response to convergence between buoyant lithospheres (15).  
48 But Indian lithosphere only reaches ~400-800 km north of the Himalayan front (9-14)  
49 and according to kinematic reconstructions of Indian plate consumption (11, 13, 16), and  
50 geological estimates of the last slab break-off in the Himalaya (17), accounts for only the  
51 last 25-13 Ma (diachronous along-strike) of India-Asia convergence (11, 16).  
52 Paradoxically, the youngest unequivocal geological records of plate-boundary-wide  
53 oceanic subduction between India and Asia are older than 60 Ma (18, 19), after which  
54 more than 5000 km of India-Asia plate convergence occurred (20, 21). So between the  
55 geologically recorded collision and the onset of horizontal underthrusting of Indian  
56 lithosphere, thousands of kilometers of post-collisional subduction occurred.

57 This paradox is not readily explained by dynamic models of continental collision.  
58 These rather portray a process of ~10 Ma, during which a few hundred kilometers of one  
59 continental margin is dragged down below another, causing deformation of both margins,  
60 after which convergence stops, the slab detaches, and the deformed belt rebounds and  
61 uplifts (22). Long-standing controversy in the geological debate on the India-Asia  
62 collision history comes from different solutions to explain this paradox. End-member  
63 solutions fall into three classes that fundamentally differ in post-collisional  
64 paleogeography of the Indian plate. The first end-member predicts that all post-collisional  
65 subduction consumed continental lithosphere (19, 23, 24), and the second and third infer  
66 that after initial collision, oceanic lithosphere remained to the north (8, 25-28), or to the  
67 south (11, 29) of the initial collision zone, which subsequently subducted 'post-collision'.  
68 The former option challenges the paradigm of continental unsubductability and if true, is  
69 key to advance understanding of mantle dynamics (24). The latter options challenge  
70 paradigms of orogenic architecture and evolution ensuing from oceanic subduction (23,

71 30) and if true, holds key lessons for reconstructing paleogeography from orogenic  
72 archives (31). In all cases, the records of magmatism, deformation, and topographic rise  
73 in Tibet and the Himalaya between the onset of collision and the onset of horizontal  
74 underthrusting occurred in context of, and contain key information on a-typical  
75 subduction, either in terms of the nature of the downgoing plate, or in terms of the  
76 orogenic and magmatic response.

77 In the last decade, the controversy on India's paleogeography has reached an  
78 impasse: each of the end-member scenarios is argued for and against based on the same  
79 types of data, notably sediment provenance constraining upper plate sediments arriving  
80 on lower plate continental margins (8, 11, 19, 27, 32, 33), paleomagnetic data  
81 constraining paleolatitudes of continental margins and arcs (27, 29, 34-37), and seismic  
82 tomographic images revealing locations of past subduction zones (13, 16, 38, 39). Even  
83 though the volume of these databases has rapidly increased in recent years, they have  
84 mostly led to repetition of these views on Indian paleogeography, and somewhat  
85 distracted from using the unique opportunities of the archetype to challenge and develop  
86 paradigms of geodynamics, orogenesis, and environmental response.

87 The aims of this paper are three-fold: (i) I first attempt at formulating the paradox  
88 and explaining the controversy and the key predictions of each proposed class of  
89 explanations; (ii) I then review geological constraints on Indian plate subduction  
90 provided by the Himalayan mountains that consist of offscraped and thrust upper  
91 crustal rocks derived from Indian plate lithosphere and on coeval upper plate geological  
92 evolution of the Tibetan Plateau; (iii) I will use these constraints to identify which  
93 tectonic and magmatic reorganizations coincide with horizontal Indian underthrusting,  
94 and aim to identify the natural laboratory to analyze the dynamics of non-sudbuctable  
95 lithosphere convergence; (iv) Finally, I will discuss ways forward to reconcile existing  
96 datasets and find novel ones to break through the impasse in Greater India  
97 paleogeography reconstruction and show the opportunities that each of the three end-  
98 member scenarios would provide in using the India-Asia archetype to constrain the  
99 geological and dynamic consequences of its a-typical post-collisional subduction.

100

## 101 Review

### 102 The paradox: underthrust versus subducted Indian plate lithosphere

103 A key question in the analysis of the India-Asia collision history and dynamics is  
104 where and how post-collisional convergence has been accommodated. Kinematic  
105 reconstructions have shown that approximately 1000-1200 km of Cenozoic convergence  
106 was accommodated by shortening and extrusion in the overriding plate of Tibet (11, 40,  
107 41). Reconstructing this convergence in the mantle reference frame aligns the southern  
108 Eurasian margin with underlying slabs imaged by seismic tomography, and in the  
109 paleomagnetic reference frame satisfies first-order vertical axis rotations and south  
110 Tibetan paleolatitudes for the Cretaceous and Paleogene (11). This reconstructed  
111 shortening of Tibet is by far the largest amount of intra-plate shortening recorded in post-  
112 Paleozoic orogens (31). Shortening records of the Indian-plate-derived thin-skinned  
113 Himalaya fold-thrust belt give somewhat smaller numbers, between 600-900 km (42). It  
114 is puzzling that post-collisional convergence far exceeds these numbers: the earliest  
115 estimates for post-collisional convergence assumed a 45 Ma collision and predicted a  
116 shortening deficit of ~1000 km (43), but stratigraphic ages of the oldest foreland basin  
117 clastics in the northernmost continental rocks of the Himalaya, as well as ages of (U)HP  
118 metamorphism in continent-derived rocks in the northern Himalaya has pushed the  
119 estimated initial collision age backward, to ~60-55 Ma (18, 44, 45). And where previous  
120 plate circuits, constrained by a few magnetic anomalies for the Indian ocean in the  
121 Cenozoic, predicted ~4500 km of post-60 Ma convergence (20), the recent high-  
122 resolution marine magnetic anomaly dataset of DeMets and Merkouriev (21) has brought  
123 this number up to well over 5000 km (Fig. 1). Much of the post-collisional subduction  
124 has thus not left an accreted rock record, either because of whole-sale subduction, or of  
125 (subduction-) erosion of previously accreted records.

126 Seismological research in the last two decades has painted a detailed image of the  
127 mantle below India and Tibet that helps identifying where lost lithosphere may now  
128 reside. First, lithosphere below Tibet is up to 260 km thick, which was at first surprising  
129 (46): major lithospheric thickening associated with intraplate shortening is predicted to  
130 lead to convective instability of lithosphere, that will then delaminate (47). However,  
131 since then the thick lithosphere below Tibet has become interpreted as horizontally

132 underthrust Indian crust and continental mantle lithosphere (9-14). Tibetan lithosphere  
133 has indeed delaminated: Indian continental crust appears to directly underlie Tibetan  
134 crust, not intervened by a thick lithospheric mantle (14). In addition, seismic tomographic  
135 evidence for bodies of high-velocity material that may represent delaminated Tibetan  
136 lithosphere have been identified in the upper mantle below the horizontally underthrust  
137 Indian lithosphere, suggesting delamination prior to underthrusting (48). Moreover,  
138 recent seismological analysis has shown that delamination is not restricted to Tibet, but  
139 also affected the Yunnan region to the southeast of the eastern Himalayan syntaxis, where  
140 a conspicuous, circular shaped hole in the continental lithosphere is underlain by a body of  
141 high-velocity material at the base of the upper mantle (49).

142         The first detailed seismological section that detected horizontally underthrust  
143 lithosphere revealed that the Indian continent protrudes ~400 km north of the southern  
144 Himalayan front (14). Since then, multiple seismic tomography models have reproduced  
145 this finding, but showed that the shape of the northern Indian margin is irregular,  
146 protruding ~800 km northward at the longitude of the eastern Himalayan syntaxis,  
147 abruptly stepping southward to the north of Bhutan, and then increasing to ~700 km  
148 again towards the longitude of the western syntaxis (Fig. 2) (9-13). An onset of horizontal  
149 underthrusting can be calculated when assuming that the body of lithosphere below Tibet  
150 is a rigid part of the Indian plate, reconstructing India-Asia convergence, and corrected  
151 for Tibetan shortening. This predicts that the onset of horizontal underthrusting started  
152 around the Himalayan syntaxes around 25 Ma, and becomes gradually younger to ~13  
153 Ma at the longitude of Bhutan (11, 16) (Fig. 3). Geological reconstructions of uplift,  
154 heating, and resulting leucogranite intrusion in the Himalayan mountain range interpreted  
155 to reflect lateral propagation of slab detachment predicted 25 Ma for the eastern- and  
156 westernmost Himalaya, gradually younging towards 13 Ma in Bhutan (17). This match  
157 suggests that the thick body of lithosphere below Tibet is indeed horizontally underthrust  
158 Indian lithosphere.

159         All Indian plate lithosphere that was consumed before Miocene horizontal  
160 underthrusting must thus have subducted into the mantle. There is broad consensus that  
161 the majority of this subducted lithosphere resides in the lower mantle below India, with a

162 smaller and younger slab that was the last to detach, overturned in the mantle to the north  
163 of the main India slab (Fig. 2) (11, 13, 38, 39, 50). An additional anomaly in the lower  
164 mantle below the equatorial Indian ocean has also long been interpreted as Neotethyan  
165 (29, 38, 39), but may instead be a relict of Mesozoic subduction between Tibetan blocks  
166 (16) (Fig. 2).

167 In summary, the paradox of the India-Asia collision is the following: there is no  
168 geological record of oceanic subduction along the width of the orogen after initial  
169 collision around 60 Ma, and the system is therefore widely believed to have been fully  
170 continental since this time (13, 23, 24); yet thousands of kilometers of Indian plate  
171 lithosphere was consumed without leaving an accretionary record, and subducted deeply  
172 into the mantle, which are both typically associated with oceanic subduction and not  
173 previously demonstrated for continents (31). Only in the early to middle Miocene,  
174 unsubductable Indian Plate lithosphere arrived in the collision zone, and horizontally  
175 underthrust the upper plate.

176

### 177 [The controversy: scenarios for Indian plate paleogeography and subduction](#) 178 [history](#)

179 The above paradox has led to paleogeographic reconstructions for post-collisional  
180 Greater India that fall into three classes (Fig. 4). The first and most commonly portrayed  
181 scenario (Model C, for Continental) assumes that all post-collisional convergence  
182 consumed continental lithosphere (19, 23, 24, 40). This scenario provides a  
183 straightforward explanation for the absence of accretion of OPS after 60 Ma in the  
184 Himalayan orogen, but requires thousands of kilometers of continental subduction, and  
185 this subduction must have been accommodated along a thrust in the Himalayas (24). The  
186 width of continental Greater India portrayed on published paleogeographic maps differs  
187 as function of collision age, plate circuit, and assumed Tibetan shortening, but predicts  
188 Gondwana reconstructions in which Greater India was conjugate to the entire western  
189 Indian margin (24) beyond the Argo Abyssal Plain (Fig. 4). This Argo Abyssal Plain is of  
190 importance because it recorded Jurassic continental break-up, around 155 Ma, well

191 before the separation of India from Australia around 130 Ma, and was thus conjugate to a  
192 different continent and plate than India: Argoland (51).

193         The second scenario (model A, for Arc) points out that between the Himalaya and  
194 continental southern Eurasia, there are ophiolites and intra-oceanic arc rocks, and invokes  
195 that the 60 Ma collision recorded arrival of the north Indian continental margin in an  
196 intra-oceanic subduction zone, followed by obduction of ophiolites and arc rocks onto the  
197 continental margin (8, 25-28, 52). Following this collision, oceanic lithosphere remained  
198 between the initial collision zone and Eurasia, which was consumed until arrival of the  
199 obducted Indian continental margin at the Tibetan trench. Because there is no  
200 accretionary record of post-60 Ma oceanic subduction, the age of this arrival is based on  
201 interpretations of changes in magmatism in Tibet, or an a (contested) youngest age of  
202 marine sedimentation in the Himalaya, at  $40\pm 5$  Ma (8, 26, 28). To explain how Tibet-  
203 derived sediments arrived at the north-Indian margin around 60 Ma, a recent modification  
204 of this model suggested that the north Himalayan ophiolites originated at the south  
205 Tibetan margin in the early Cretaceous, but migrated southward, together with overlying  
206 Tibet-derived sediments, due to opening of a back-arc basin (8). The intra-oceanic arc  
207 scenario thus predicts that part of the post-collisional subduction history consumed  
208 oceanic lithosphere that must have subducted along a trench between the Himalayan  
209 ophiolites and the south Tibetan margin. Additionally, the assumed  $40\pm 5$  Ma collision  
210 age of the obducted Indian margin and Tibet would still require large amounts ( $\sim 1000$ -  
211  $2000$  km at the longitude of Bhutan) of continental subduction prior to horizontal  
212 underthrusting (Fig. 4). The reconstructed width of continental Greater India depends on  
213 the assumed collision age with Tibet, but would bring the north Greater Indian margin  
214 adjacent to most of the west Australian margin up to the Argo Abyssal Plain.

215         The third scenario (model M, for Microcontinent) invokes that the 60 Ma  
216 collision in the north Himalaya involves a Tibetan Himalayan microcontinent that rifted  
217 and drifted away from Greater India in Cretaceous times, opening a conceptual Greater  
218 India Basin (GIB) ocean in its wake (29). Assuming that the horizontally underthrust  
219 portion of India below Tibet represents the southern paleo-passive margin of this basin  
220 leads to a reconstruction whereby Greater India in Gondwana times did not extend



221 beyond the Wallaby Fracture Zone of the southwest Australian margin (11), far south of  
222 the Argo Abyssal Plain, but consistent with west Australian margin reconstructions that  
223 interpreted that Jurassic break-up of Argoland to continue to the Wallaby Fracture Zone  
224 (51). This model thus invokes that continental subduction was restricted to only the lower  
225 crustal and mantle underpinnings of the Tibetan Himalayan microcontinent. However,  
226 this model also requires that an oceanic basin was consumed along a thrust within the  
227 Himalayan mountain range without leaving a modern geological record anywhere in the  
228 Himalaya. Finally, this scenario does not require, but also does not exclude the intra-  
229 oceanic arc scenario of Model A – this would merely change the width of the GIB.

230           Each of these scenarios explains some first-order observations from the Greater  
231 Indian paradox, and satisfies some long-held paradigms in subduction behavior or  
232 orogenesis, but challenges others. And each of these models has been defended as well as  
233 contested based on paleomagnetic, structural geological, stratigraphic, and seismic  
234 tomographic data. Below, I will briefly review the geological architecture of the  
235 Himalaya and Tibet that is relevant to identify future research targets to advance the  
236 discussion, and to identify the main geological and geodynamic phenomena that occurred  
237 in the time window of horizontal Indian underthrusting.

238

### 239 **The constraints: architecture and evolution of the Tibetan-Himalayan orogen**

240           Elements of the Himalayan and Tibetan orogen that play a key role in the  
241 interpretations of its tectonic history since 60 Ma are (i) the accretionary fold-thrust belt  
242 of the Himalaya that was offscraped from now-underthrust/subducted Indian plate  
243 lithosphere ; (ii) a belt of overlying ophiolites, and in the west of the collision zone,  
244 Cretaceous-Eocene intra-oceanic arc rocks that represent the upper plate of an overriding  
245 oceanic lithosphere above a subduction zone; and (iii) continental crust of the Tibetan  
246 plateau that consists of pre-Cenozoic accreted terranes and intervening sutures, intruded  
247 by a Mesozoic-Cenozoic magmatic arc that also shows it was in an upper plate position  
248 above a subduction zone (Fig. 5). Below, I summarize these constraints and briefly  
249 indicate how they play a role in the three scenarios for Indian paleogeography  
250 summarized above.

251

252 **Himalaya**

253         The accretionary fold-thrust belt of the Himalaya consists continent-derived  
254 nappes that underlie of ocean-derived accreted units. These accreted rock units play a key  
255 role in reconstructing subducted plate paleogeography. Conceptually, accreted rock units  
256 fall into two broad types: ocean-derived units consist of Ocean Plate Stratigraphy (OPS),  
257 comprising pillow lavas (MORB, OIB, IAT), pelagic oceanic sediments, and foreland  
258 basin clastics (53). Continent-derived units consist of Continental Plate Stratigraphy  
259 (CPS) that in its simplest form comprises slivers of a basement from an earlier orogenic  
260 cycle, an unconformable cover of syn-rift elastic sediments and volcanics, shallow- to  
261 deep-marine platform to pelagic passive margin carbonates and occasional clastic series,  
262 and foreland basin clastics, although a more complex stratigraphic architecture may form  
263 due to climatic or relative sea level variation or a more complex rifting history of the  
264 continental margin (31). Key for analyzing the collision and accretion history are the  
265 foreland basin clastics: these not only date arrival of the accreted units at a trench, but  
266 also allow fingerprinting the nature of the overriding plate through sediment provenance  
267 analysis. The moment of accretion of thrust slices is bracketed between the youngest  
268 flysch deposits giving a maximum age and, if burial was deep enough, the age of  
269 metamorphism (in subduction setting normally of HP-LT type, except during subduction  
270 infancy, when HT-HP metamorphic soles may form (54)) of the accreted units, which  
271 gives a minimum age (31). Finally, in fold-thrust belts with continuous foreland-  
272 propagating thrusting in which almost all subducted lithosphere left its upper crust in the  
273 orogen, the youngest age of foreland basin clastics in the higher nappe tends to be similar  
274 to the oldest age of foreland basin clastics in the next-lower nappe (as for instance in the  
275 Apennines and Hellenides of the Mediterranean region (55)). Conversely, extended  
276 periods of non-accretion and wholesale subduction, or subduction erosion removing  
277 previously accreted rocks, are revealed by age gaps between foreland basin clastics in  
278 adjacent nappes (e.g., in the Japan accretionary prism (53)).

279         The Himalayan fold-thrust belt is commonly divided into four main units, three of  
280 which follow the logic outlined above. The highest units, located below the Indus-  
281 Yarlung ophiolites is a *mélange* that consists of deformed and in places metamorphosed

282 OPS. These include pillow basalts, cherts that are not older than Triassic in age reflecting  
283 the age of opening of the Neotethys ocean (56), and foreland basin clastics in which the  
284 youngest recognized ages are ~80 Ma (57). The first-accreted units are dismembered  
285 metamorphic sole rocks with ~130 Ma  $^{40}\text{Ar}/^{39}\text{Ar}$  cooling ages that provide a minimum  
286 age for subduction initiation (58). HP-LT metamorphic OPS units found in the *mélange*  
287 below the ophiolites interpreted to have formed during oceanic subduction have ages of  
288 100-80 Ma (45).

289         This OPS-derived *mélange* overlies the Tibetan Himalayan nappe. This nappe  
290 consists of Paleozoic basement, upper Paleozoic syn-rift clastics and volcanics, a  
291 carbonate-dominated passive margin sequence that continues into the Cenozoic (59), and  
292 Paleocene to lower Eocene foreland basin clastics whose age estimates range from ~61-  
293 54 Ma (18, 19, 60). Metamorphic ages of (U)HP-metamorphic, deeply underthrust  
294 equivalents of the Tibetan Himalaya reveal ages suggesting that burial was underway by  
295 57 Ma (45). These records provide evidence that continental lithosphere on the Indian  
296 plate arrived in a subduction zone by ~60 Ma or shortly thereafter.

297         The Tibetan Himalayan nappes overlie crystalline rocks of the Greater Himalaya.  
298 These Greater Himalayan rocks are atypical for accretionary fold-thrust belts in their  
299 metamorphic grade as well as their stratigraphy. They consist of Paleozoic pre-  
300 Himalayan crystalline basement and sediments that were metamorphosed in Cenozoic  
301 times under high-grade metamorphic conditions, up to partial melting, and intruded by  
302 leucogranites (8, 61-63). These rocks underwent prograde metamorphism from ~50 Ma  
303 onward showing they have been part of the orogen since at least early Eocene time (61,  
304 64). The Greater Himalayan sequence is separated from the overlying Tethyan  
305 Himalayan sequence by the South Tibetan Detachment (STD), a normal fault that has  
306 been active in latest Oligocene to middle Miocene time (61) and that represents a tectonic  
307 omission (62) (Fig. 6). No Mesozoic stratigraphy or Cenozoic foreland basin clastic  
308 sequences are known from the Greater Himalaya (8, 63). These may either have been cut  
309 out by the South Tibetan detachment, which would make the Greater Himalaya a separate  
310 nappe derived from crust that was paleogeographically to the south of the Tibetan  
311 Himalaya and that underthrust below the Tethyan Himalaya in the early Eocene, or it

312 formed the original stratigraphic underpinnings of the Tethyan Himalaya making them  
313 part of the same nappe.

314           The base of the Greater Himalaya is the Main Central Thrust (MCT) a ductile  
315 shearzone with a downward decreasing metamorphic grade, signalling syn-exhumation  
316 activity, that reveals ages of latest Oligocene to middle Miocene (~26-13 Ma) activity  
317 coeval with the South Tibetan Detachment (61, 62). The coeval activity of the MCT and  
318 STD is commonly interpreted to reflect extrusion of a mid-crustal part of the orogen (65)  
319 that slowly heated up following burial since the Eocene (61). During Miocene extrusion,  
320 the Greater Himalayan crystalline rocks were emplaced onto the Lesser Himalayan  
321 sequence that contain Lower Miocene foreland basin clastics (see below) and were  
322 accreted to the orogen afterwards. There is no geological record of fault zones of Eocene  
323 to Miocene age between the Greater and Lesser Himalaya, and the MCT does not appear  
324 to reactivate an such a structure (23).

325           The Lesser Himalaya consists of a Paleozoic and older, low-grade  
326 metasedimentary, and discontinuous Cretaceous to Paleocene clastic sedimentary rocks,  
327 in places overlain by Eocene and Miocene foreland basin clastics (60). Upper Cretaceous  
328 to Eocene clastic sedimentary rocks become more prominent towards the west, in  
329 Pakistan, where Eocene and younger foreland basin clastics are also found on the  
330 undeformed Indian continent (33, 66, 67). The provenance of Upper Cretaceous and  
331 Eocene foreland basin clastics in the Lesser Himalayas and on the NW Indian continent  
332 reveal erosion of Indian margin rocks and ophiolites that signal Eocene or older  
333 obduction, and is commonly interpreted to reflect collision recorded in the Tethyan  
334 Himalaya to the north (33, 60, 66, 67). However, the western margin of India was also  
335 the locus of orogenesis due to ophiolite emplacement, in a Late Cretaceous and an  
336 Eocene phase, but this obduction was governed by convergence between the Indian and  
337 Arabian plates and the collision of the Kabul microcontinent with west India (68, 69). So  
338 far, the sediment provenance studies have not identified whether the west and north  
339 Indian margin have distinctly different signatures presenting an unresolved challenge in  
340 interpreting sediment provenance (11). Duplexing of the Lesser Himalayan rocks

341 occurred in the last ~15-13 Ma and accounted for hundreds of kilometers of shortening  
342 that is similar to contemporaneous Indian plate consumption (42, 70).

343 The structure of the Himalaya summarized above show an overall foreland  
344 propagating fold-thrust belt, but with a clear omission of accretion between the Eocene  
345 (Tibetan and Greater Himalaya) and Miocene (Lesser Himalaya). There are two end-  
346 member interpretations of this hiatus in accretionary record. Before their Miocene  
347 emplacement onto the Lesser Himalaya, the rocks exposed in the Greater Himalaya must  
348 have been overlying rocks that have now been transported farther below the orogen and  
349 the nature of these rocks is unknown. On the one hand, these rocks may have been the  
350 original underlying Indian basement (23, 70) (Fig. 7). In that case, there has been no net  
351 convergence between the Greater and Lesser Himalaya between Eocene burial of the  
352 former and Miocene burial of the latter. The Eocene-Miocene India-Asia plate boundary  
353 must then have been located north of the Himalaya. Of the three models for Indian  
354 paleogeography (Fig. 4), only Model A (intra-oceanic arc) could allow for this scenario:  
355 in that case, early Eocene burial of the Greater Himalaya follows upon obduction, and  
356 activation of the MCT would reflect final collision of the obducted margin with Tibet –  
357 but this would require a diachronous Miocene collision age, instead of the proposed  $40\pm 5$   
358 Ma collision ages. All other scenarios require that a subduction plate boundary (intra-  
359 continental, or ocean-below continent) existed within the Himalaya. In that case, the  
360 Greater Himalayan sequence must have decoupled from its Indian basement sometime  
361 after its early Eocene arrival in the orogen, and subsequently formed part of a slowly  
362 thickening and heating orogen. In that case, the activation of the MCT displaced the  
363 modern Greater Himalayan from a deeper part of the orogen and emplaced it onto the  
364 Lesser Himalayan foreland. Such a scenario is typically implied in numerical simulations  
365 of Himalayan extrusion and channel flow (71) and interprets the MCT as an out-of-  
366 sequence thrust. Importantly any Eo-Oligocene accretionary record and associated thrusts  
367 that formed below the Greater Himalayan sequence were then removed from the orogen  
368 through subduction erosion upon activation of the MCT (Fig. 7). In Model C and A, this  
369 removed part of the orogen consisted of accreted CPS, in Model M (microcontinent), it  
370 may also have included OPS.

371

372 Indus-Yarlung ophiolites and Kohistan-Ladakh arc

373 Overlying the accretionary orogen of the Himalaya are a series of ophiolites  
374 concentrated in a narrow belt along the northern Himalaya (8) (Figs. 5 and 6). These  
375 'Indus-Yarlung' ophiolites are predominantly Early Cretaceous in age (~130-120 Ma),  
376 during which time they formed by extension in the forearc above a (presumably  
377 incipient) subduction zone (8, 58). In some places also older, Jurassic oceanic crust is  
378 found in ophiolites, which may reflect the ocean floor trapped above the subduction zone  
379 in which the Cretaceous ophiolites formed (8). In addition, in the western Himalaya, a  
380 long-lived intra-oceanic arc sequence (150-50 Ma) that is located between the ophiolites  
381 and the continental units of southern Eurasia is known as the Kohistan-Ladakh arc (72).  
382 These sequences showed that the accretion of the Himalayan rocks occurred below a  
383 forearc that consisted of oceanic lithosphere, which plays a central role in the controversy  
384 about Greater Indian paleogeography.

385 The Kohistan-Ladakh arc is overlain by a Cretaceous to Eocene sedimentary  
386 sequence and is separated from Tibetan continental rocks by the Shyok Suture (Fig. 5).  
387 Convergence across this suture zone has been proposed to be either significant and  
388 continuing to Eocene time (27, 28) or minor and pre-dating the late Cretaceous (32), but  
389 in any case testifies to the existence of a paleo-subduction zone between the Kohistan-  
390 Ladakh arc and Eurasia. The Indus-Yarlung ophiolites are overlain by sediments of the  
391 Xigaze forearc basin that form a major syncline with 4-5 km of sediments along 550 km  
392 of the subduction zone (73, 74). The oldest sediments are ~130 Ma old and  
393 unconformably overlie exhumed oceanic core complexes of the ophiolites and elsewhere  
394 interfinger with the ophiolites' pelagic sedimentary cover (75), and the youngest part of  
395 the continuous section is ~50 Ma (73, 74). Low-temperature thermochronology revealed  
396 that the succession may have been almost twice as thick and suggested that sedimentation  
397 and burial may have continued until ~35 Ma (73). The Xigaze forearc has been shortened  
398 along the north-dipping Gangdese Thrust, which brought Tibetan rocks over the forearc  
399 between ~27 and 23 Ma (76), and the Great Counter thrust that backthrusted the Xigaze  
400 forearc over the south Tibetan margin between ~25 and 17 Ma (8) (Fig. 6). Sediment

401 provenance studies of the Xigaze forearc sequence typically depict southern Tibet and its  
402 overlying magmatic arc as source (73-75), although others prefer an intra-oceanic arc  
403 derivation (26, 27) and there is no known accretionary record of OPS or melange along  
404 the strike of the Xigaze forearc basin that may reflect the location of a post-60 Ma  
405 paleosubduction zone.

406         The Indus-Yarlung ophiolites have been interpreted as the forearc of the Eurasian  
407 plate, whereby they formed by (hyper)-extension of the Tibetan continental lithosphere,  
408 occasionally trapping ocean floor that existed before subduction initiation next to the  
409 south Tibetan passive margin (77, 78). In this case, the Kohistan-Ladakh arc forms an  
410 along-strike, offshore continuation of a contemporaneous arc in Tibet (the Gangdese arc,  
411 Fig. 6) and the Shyok suture accommodated only minor convergence that eastwards was  
412 accommodated within the Tibetan Plateau (11, 32). This scenario is required by Model C  
413 (fully-continental Greater India), and preferred by model M (microcontinent). On the  
414 other hand, Model A predicts that the Kohistan-Ladakh arc and Indus-Yarlung ophiolites  
415 formed at (or migrated to (8)) equatorial latitudes, far south of the south Tibetan margin,  
416 at a separate subduction zone (26-28) from the south Tibetan active margin. This model  
417 predicts major convergence across the Shyok Suture, but requires that a long-lived  
418 subduction zone is hidden between the Xigaze Basin and the adjacent south Tibetan  
419 margin.

420

#### 421 Tibetan Plateau

422 The Tibetan Plateau consists of a series of Gondwana-derived continental fragments and  
423 intervening suture zones that amalgamated in Mesozoic time (8, 79). The southernmost of  
424 these fragments is the Lhasa Block that accreted to the Tibetan Plateau in early  
425 Cretaceous time (8, 79), around the same time as the formation of the south Tibetan  
426 ophiolites above a nascent subduction zone to the south of Lhasa (58). Shortening of the  
427 Tibetan upper plate above this subduction zone already started in late Cretaceous time,  
428 and amounted perhaps already 400 km before initial collision (41, 80, 81) in addition to  
429 the 1000-1200 km of post-60 Ma shortening (11, 41). Detailed stratigraphic records  
430 reveal that shortening in the plateau may have been pulsed, but there is no evidence of a

431 shortening pulse associated with initial collision around 60 Ma; the recorded pulses may  
432 rather reflect changes in Indian subduction rate (21, 81). In Eocene-Oligocene time,  
433 shortening was concentrated in the central Tibetan Plateau. Sometime in late Eocene or  
434 Oligocene time ( $\sim 30 \pm 7$  Ma), Tibetan shortening started to affect the southern margin of  
435 the rigid Tarim block to the north of the modern Plateau. To the west of this block,  
436 Eurasian lithosphere started to subduct southward, accommodated along the Kashgar-  
437 Yecheng transform fault, whereas to the southeast of Tarim, Tibetan crust started to move  
438 NE-ward along the Altyn Tagh fault (82). In late Oligocene time,  $\sim 25$  Ma, shortening  
439 propagated beyond the Tarim block into the Tien Shan, intensifying at  $\sim 13$ -10 Ma (83).  
440 Throughout this history, also NE Tibet underwent outward growth by foreland-  
441 propagating thrusting (8, 84).

442 Paradoxically, even though the Tibetan Plateau and Tien Shan underwent ongoing  
443 shortening in Oligocene to Early Miocene time, south-central Tibet experienced dynamic  
444 subsidence, or even extension. On the southern margin of the Lhasa block, close to the  
445 suture zone, formed the 1300 km long Kailas Basin, which forms a southward thickening  
446 wedge of  $>3$  km of sediments whose architecture and sedimentology suggests it formed  
447 in the hangingwall of a north-dipping normal fault, even though the fault itself is not  
448 exposed, perhaps cut out by the Great Counter Thrust (85, 86) (Fig. 6). The stratigraphy  
449 in any section of the basin accumulated within only 2-3 Ma, but the timing of basin  
450 formation propagates diachronously along-strike, between 26 and 24 Ma in the west, and  
451 becoming as young as 18 Ma in the east (86).

452 Upper plate deformation also involved lateral extrusion (40). In the east of the plateau,  
453 crust was extruded eastwards already in the Eocene, first accommodated by rotations and  
454 thickening in northwest Indochina and later, sometime between  $\sim 30$  and 15 Ma also by  
455 motion of entire Indochina along the Red River Fault (87) (Fig. 5). In western Tibet, a  
456 similar process may have played a role, although the lack of detailed knowledge of the  
457 geology of Afghanistan limits constraints (25). A recent reconstruction of Central Iran  
458 (88) pointed out major late Cretaceous to Eocene mobility and E-W convergence across  
459 the east Iranian Sistan suture requires that continental fragments of Afghanistan may have  
460 undergone major westward displacement (Fig. 5). Restoring such displacement would



461 bring the Aghanistan fragments north of the Kohistan-Ladakh arc and is thus relevant in  
462 interpreting its paleolatitudinal history in terms of Greater Indian paleogeography, but  
463 awaits future detailed constraints.

464 Around 15-10 Ma, a prominent change in deformation of the Tibetan Plateau occurred,  
465 which most famously marks the onset of regional E-W extension in the plateau interior  
466 (89, 90) (Fig. 6). Towards the west, this extension is bounded by the Karakoram Fault  
467 that accommodated ongoing convergence in the Pamir region (41) (Figs. 5 and 6) and to  
468 the east, it is accommodated by E-W shortening in the Longmenshan range, and by a  
469 deflection of motion towards the Yunnan region in the southeast, accommodated along  
470 major strike-slip faults (3, 90). This motion is prominent today as reflected by GPS  
471 measurements. Eastward surface motion components increase from near-zero at the  
472 Karakoram Fault eastward to a maximum of ~2 cm/yr on the central plateau (91).  
473 Eastward motion components then decrease further to the east due to an increasing  
474 southward velocity component in eastern Tibet, as well as E-W shortening in the  
475 Longmenshan (90, 91). The extension of the plateau interior and the motion of crust  
476 towards the southeast is widely interpreted as driven by excess gravitational potential  
477 energy resulting from plateau uplift (3, 47), facilitated by a partially molten middle crust  
478 (92). The trigger of extension is thought to reflect middle Miocene uplift of Tibet due to  
479 lithospheric delamination (3, 47, 90), or due to Indian continental underthrusting (15).

480 Finally, the Lhasa terrane contains the prominent Gangdese batholith that  
481 represents a long-lived volcanic arc (8) (Fig. 6). Arc magmatism in the Lhasa terrane  
482 related to Neotethys closure has been active since at least early Cretaceous time and  
483 perhaps longer (8). Magmatism of the Gangdese arc since early Cretaceous time  
484 contained flareups and periods of reduced activity, but was mostly active until ~45-40  
485 Ma, after which there was a lull until 25 Ma (5, 8). During this lull, potassic and  
486 ultrapotassic magmatism was active in the Qiangtang terrane, hundreds of kilometers to  
487 the north of the Gangdese batholith, after which magmatism resumed in the Lhasa  
488 terrane, ultrapotassic or shoshonitic/adakitic in composition (5, 8), associated with  
489 economic porphyry copper deposits (6). Since 20 Ma such magmatism also resumed in  
490 the Qiangtang and adjacent Songpan Garzi zones of the Tibetan Plateau (5). Interestingly,

491 this Miocene magmatism in the Lhasa terrane migrated eastward, 25-20 Ma in western  
492 Tibet but 15-10 Ma in the east, towards the longitude of Bhutan (7). The chemistry of  
493 these magmatic rocks is interpreted to be mostly derived from a previously subduction-  
494 enriched asthenospheric source that became stirred by the underthrusting continental  
495 Indian lithosphere (5-7).

496

## 497 Discussion

### 498 Opportunities, 1: Natural laboratory of converging unsubductable lithospheres

499 The kinematic reconstruction constraining of horizontal continental underthrusting of the  
500 Indian continent below Tibet identifies (only) the Miocene and younger history of the  
501 Tibetan-Himalayan geological history as natural laboratory for the convergence of  
502 unsubductable lithospheres. While and extensive analysis of the dynamics of this system  
503 is beyond the scope of this paper, several first-order temporal and spatial relationships  
504 between horizontal underthrusting and geological evolution are clear and may be used as  
505 basis to discern between existing hypotheses, or develop new.

506 Most importantly, the irregular shape of the seismically imaged northern Indian  
507 continental margin shows that initial horizontal underthrusting must have been  
508 diachronous: the coinciding age estimates from the kinematic restoration of this margin  
509 (16) (Fig. 3) and geological estimates of the youngest phase of slab break-off from the  
510 Himalaya (17) of ~25 Ma at the Himalayan syntaxes, decreasing to ~13 Ma in at the  
511 longitude of Bhutan, may provide means to discern between the effects of horizontal  
512 underthrusting and unrelated events. For instance, the re-initiation of magmatism between  
513 25 and 8 Ma in the Lhasa terrane follows the same age progression, lending independent  
514 support to the interpretation that magmatism resulted from incipient Indian continental  
515 lithosphere plowing through and stirring of a previously subduction-enriched  
516 asthenosphere (5-7, 93). On the other hand, Miocene magmatism farther north in the  
517 Tibetan plateau that started around 20 Ma is located far away from the horizontally  
518 underthrusting northern Indian continental margin, and does not show a lateral age  
519 progression, making a direct link unlikely.

520 The formation and deposition of the Kailas basin follows the same diachronous trend, but  
521 precedes the reconstructed slab break-off by a few Ma (86). The recognition of  
522 diachronous initial horizontal underthrusting allows explaining this trend, as well as the  
523 apparent paradox of N-S extension in the Kailas Basin of southern Tibet (85, 86) and the  
524 coeval ongoing upper plate shortening in the Pamir, along the Altyn Tagh fault, and in  
525 NE Tibet (82, 84). The subsidence of the Kailas basin is well explained as the result of  
526 negative dynamic topography, or even upper plate extension, caused by the Himalayan  
527 slab resisting slab advance, just prior to its detachment (16, 86, 94) (Fig. 8). This  
528 resistance only occurs where the slab is still attached, explaining the diachroneity in  
529 Kailas Basin formation and its subsequent uplift. But where slab detachment has already  
530 occurred, i.e. at the longitude of the Himalayan syntaxes, the Pamir and eastern Tibet,  
531 horizontal Indian underthrusting may already have caused enhanced friction to drive the  
532 apparently paradoxical simultaneous upper plate shortening and extension (Fig. 8).

533 The reconstructed horizontal Indian underthrusting also sheds light on the long-standing  
534 debate on the trigger of E-W extension in Tibet. There is widespread consensus that this  
535 extension reflects the gravitational collapse of the Tibetan Plateau (3, 15, 47, 90),  
536 whereby as final trigger, lithosphere delamination of south-central Tibet (3, 47, 90) or  
537 uplift due to horizontal Indian underthrusting (15) have been suggested. Horizontally  
538 underthrust Indian continental lithosphere directly underlies Tibetan crust, and its  
539 lithospheric mantle must thus have delaminated prior to the 25 Ma onset of horizontal  
540 underthrusting in western and eastern Tibet. In addition, not only the source area below  
541 the Tibetan Plateau, but also the 'sink' of Middle Miocene and younger crustal motion in  
542 the Yunnan region has undergone lithospheric delamination (49). This suggests that the  
543 15-10 Ma onset of E-W extension was likely not triggered by delamination. More likely,  
544 collapse was driven by the final onset of horizontal underthrusting below the entire  
545 plateau following final slab break-off (15). If horizontal underthrusting indeed caused  
546 uplift, the easternmost part of the Indian continental promontory north of the eastern  
547 syntaxis may have first formed a barrier against plateau collapse, which was only  
548 overcome after the entire Tibetan Plateau became horizontally underthrust by India since  
549 middle Miocene time.

550 Also middle Miocene changes in the Himalaya may be studied in context of the transition  
551 from subduction to horizontal underthrusting. Webb et al. (17) already interpreted syntaxis  
552 formation and Himalayan oroclinal bending as result of the change to horizontal  
553 underthrusting. Also the transition from extrusion of the Greater Himalayan crystalline  
554 rocks along the STD and MCT, to duplexing of the Lesser Himalayan nappes appears to  
555 coincide with the transition to horizontal underthrusting, but future analyses may test  
556 whether there was diachroneity in these processes. The coincidence of intraplate  
557 deformation events, e.g. in the Tien Shan with the onset of horizontal underthrusting in  
558 western Tibet around 25, and along the entire Tibetan margin around 13 Ma, may suggest  
559 a causal relationship linking convergence between unsubductable lithosphere to intraplate  
560 deformation. On the other hand, the shortening in the Tien Shan may also be a natural  
561 northward progression of intraplate deformation that had long been ongoing in the  
562 Tibetan plateau. Future numerical experiments may test such dynamic hypotheses built  
563 on the Miocene Tibetan-Himalayan natural laboratory for the convergence of  
564 unsubductable lithosphere.

565

## 566 [Opportunities, 2: Improving methodology to unlock the post-collisional](#) 567 [subduction laboratory](#)

568 The ongoing controversy of Greater Indian paleogeography currently hampers using the  
569 interval between initial collision, around 60 Ma, and the 25-13 Ma of horizontal Indian  
570 underthrusting as a conclusive natural laboratory for post-collisional subduction.

571 Regardless of which of scenarios of Model C, A, or M will turn out to be correct, if any,  
572 this natural laboratory holds great promise. Models C and A so far offer no explanation  
573 for why there was a transition from subduction to horizontal underthrusting, or what  
574 caused the diachroneity of that transition, but if these scenarios are correct, that  
575 explanation must provide a unique constraint on the subductability of continental  
576 lithosphere. Moreover, Models C and A predict that continental subduction is also  
577 possible without preservation of upper crustal units, or with large-scale subsequent  
578 removal of accreted continental crust through subduction erosion. If these models are  
579 correct, it is thus possible that paleogeographic reconstructions strongly underestimate

580 the paleogeographic area occupied by continental lithosphere. In fact, if large portions of  
581 continental lithosphere can subduct without leaving a geological record, accreted  
582 geological records such as in the Tibetan Himalaya cannot provide conclusive constraints  
583 on initial collision, but only give a minimum age (31). Finally, model C (since 60 Ma)  
584 and model A (since  $40 \pm 5$  Ma) would provide the opportunity to calibrate magmatic  
585 responses to continental subduction.

586 The subduction history of model M is entirely on par with current geodynamic  
587 paradigms, with a short-lived, late Paleocene to early Eocene phase of microcontinental  
588 lower crust and mantle lithosphere subduction combined with upper crustal accretion that  
589 is well-documented elsewhere (55) and found plausible in numerical experiments (95). In  
590 model M, upper crustal nappes of all subducted or horizontally underthrust continental  
591 lithosphere still remain in the Himalayan orogen (11). The transition from subduction to  
592 horizontal underthrusting in model M is simply caused by the change from oceanic to  
593 continental subduction. But model M invokes that the anomalous magmatic history of  
594 Tibet between 45 and the 25 Ma onset of horizontal underthrusting occurred during  
595 oceanic (perhaps flat slab (11, 86)) subduction and would thus allow calibrating possible  
596 magmatic arc expressions of anomalous oceanic subduction.

597 The three models provide strongly different boundary conditions and have far-reaching  
598 consequences for the analysis of the dynamic drivers of upper and intraplate deformation,  
599 the causes of rapid plate motion changes of India, or the causes and paleogeographic  
600 context of terrestrial biota exchange and radiation. It is therefore important to attempt at  
601 breaking through the impasse in Greater Indian paleogeography reconstruction. I will  
602 attempt at briefly identifying where opportunities may lie to achieve this.

603 The only quantitative constraint on paleogeographic position comes from paleomagnetic  
604 data providing paleolatitudinal control. Paleomagnetic analyses on rocks derived from  
605 Greater India such as the Tibetan Himalayan sequence, of ophiolites and intra-oceanic  
606 arcs and their cover, and of the Lhasa terrane of southern Tibet in principle allows  
607 discerning between Model C, A, and M. But each of these models has been defended and  
608 and challenged based on paleomagnetic data (27, 29, 34-37). So are paleomagnetic data  
609 inconclusive? Rowley (34) recently pointed out that the widely used method to compare

610 paleomagnetic study means ('paleopoles') with apparent polar wander paths that provide  
611 the global reference against which these data are compared and that are based on  
612 averages of study means, is indeed barely conclusive. The paleopoles underlying APWPs  
613 are scattered by  $\sim 20^\circ$  around the mean, and Rowley (34) argued that individual  
614 paleopoles cannot constrain paleolatitude at a higher resolution. Vaes et al. (96),  
615 however, recently analyzed the source of this scatter, and showed that alongside common  
616 paleomagnetic artifacts such as undersampling of paleosecular variation, and inclination  
617 shallowing in sediments, scatter is mostly caused by the degree to which paleosecular  
618 variation is averaged: scatter is a function of the number of paleomagnetic datapoints  
619 used to determine a paleopole. And because this number is arbitrary, the statistical  
620 properties of APWPs calculated from paleopoles are arbitrary. Vaes et al. (96) provided a  
621 way forward in which paleopoles are compared to a reference curve that is also calculated  
622 from paleomagnetic readings rather than paleopoles, and developed a comparison metric  
623 that demonstrates a paleolatitudinal difference or vertical axis rotation with 95%  
624 confidence. This would provide a means to compare datasets of unequal magnitude and  
625 propagate uncertainties, and may provide a more conclusive, quantitative, and robust  
626 paleomagnetic analysis that may discern between the Greater Indian paleogeography  
627 models.

628 Models C, A, and M each invoke that a plate boundary must have existed south of the  
629 Tibetan Plateau between the Paleocene to Early Eocene accretion of the Tibetan and  
630 Greater Himalayan units in the orogen, and the accretion of the Miocene Lesser  
631 Himalayan units. If this plate boundary was located in the Himalayas during all or some  
632 of the period between 60 and 25/13 Ma, as currently required by all three scenarios, there  
633 may be no record due to out-of-sequence thrusting along the MCT removing the pre-  
634 Miocene underpinnings (Fig. 7). But this refocuses the attention on the process of  
635 extrusion and channel flow, this time not to explain the presence of the Greater  
636 Himalayan rocks in the orogen, but to explain the absence of its pre-Miocene  
637 underpinnings. In addition, Models C and A require that a subduction plate boundary was  
638 present between the Xigaze forearc and underlying ophiolites, and the Lhasa terrane (8).  
639 Detailed mapping, or identifying structures that could explain the lack of a record such as

640 I argue for the MCT (Fig. 7), may establish whether, when, and where such a subduction  
641 zone may have existed.

642 Also sediment provenance studies have been used to argue for and against Models C, A,  
643 and M. Part of this may underlie the qualitative nature of comparing e.g. detrital  
644 geochronology peaks between the sedimentary record of a sink and a suspected source  
645 area, and recently developed quantitative approaches that identify the likelihood of the  
646 contribution of a given source area to a sediment may advance the discussion (97). In this  
647 analysis, the range of possible source areas for sediments, particularly for Eocene  
648 stratigraphic records in the NW Lesser Himalaya and the Pakistani foreland should  
649 include not only the Himalaya-Kohistan-Ladakh-Tibetan orogen at the India-Asia plate  
650 boundary, but also the Sulaiman-Kabul Block orogen and associated ophiolites that  
651 formed independently at the India-Arabia plate boundary (68, 69) (Fig. 4).

652 Seismic tomographic records of subducted slabs are useful in identifying regions of  
653 paleo-subduction (38, 39), although global correlations suggest that the lower mantle  
654 hosts slabs of the last ~250 Ma (50). Analysis of mantle structure should hence be done  
655 in context of Mesozoic and Cenozoic subduction history and uncertainties therein (16)  
656 (Fig. 2). Nonetheless, a recent seismological study of a slab below Kamchatka was able  
657 to identify thick crust, on the order of 20 km, in a lower mantle slab (98). Once a slab can  
658 be firmly tied to lithosphere that subducted after initial collision, such as the overturned  
659 Himalayan slab that straddles the transition zone (13, 38), such seismological analyses  
660 may provide novel constraints on their composition and crustal nature.

661 In summary, on the one hand, the current controversy on Indian paleogeography  
662 stemming from the inability of geological and geophysical techniques to conclusively  
663 identify between vastly different paleogeographic scenarios, stands in the way of using  
664 the India-Asia collision zone to calibrate the geological and dynamic responses to post-  
665 collisional subduction. On the other hand, this controversy provides the opportunity (and  
666 requires) to question and improve geological methodology to constrain paleogeography,  
667 including orogen structure, sediment provenance analysis, and paleomagnetism. Solving  
668 those issues have impact far beyond the analysis of the India-Asia collision history.

## 670 Conclusions

671 Seismological images reveal that 400-800 km of Indian continental lithosphere is  
672 currently horizontally underthrust below Tibet. Using plate reconstructions that  
673 incorporate Tibetan shortening predict that the onset of horizontal underthrusting started  
674 around 25 Ma around the Himalayan syntaxes, gradually younging to 13 Ma at the  
675 longitude of Bhutan. This reconstruction coincides with independent estimates of  
676 diachronous slab break-off in the Himalaya, and identifies the Miocene history of Tibet  
677 as a natural laboratory for convergence of unsubductable lithospheres. This time period  
678 was marked by major changes in accretionary style in the Himalayas, including the  
679 extrusion of the Greater Himalayan crystalline rocks and the transition to Lesser  
680 Himalayan duplexing, but also by the onset of E-W extension and collapse of the Tibetan  
681 Plateau, and upper plate shortening reaching as far north as the Tien Shan. Also marked  
682 changes in magmatism in southern Tibet, and associated economic mineralizations  
683 spatially and temporally correlate with the reconstructed inception horizontal  
684 underthrusting. These processes may provide key ingredients of the natural laboratory for  
685 convergence of unsubductable lithosphere. Importantly, lithospheric delamination of  
686 Tibet, often cited as potential trigger for Miocene Tibetan uplift and collapse, must  
687 instead have occurred prior to horizontal Indian underthrusting, hence before the  
688 Miocene.

689 Between initial collision recorded in the Himalaya at 60 Ma and the onset of horizontal  
690 Indian underthrusting, thousands of kilometers of subduction consumed Indian plate  
691 lithosphere. I discuss three end-member scenarios that invoke that all or part of this  
692 lithosphere was continental, challenging geodynamic and paleogeographic reconstruction  
693 paradigms, or that most of this lithosphere was oceanic, challenging magmatic and  
694 orogenic architecture paradigms. But an impasse is reached because each of these  
695 reconstructions is argued for and against based on the same datatypes. I identify  
696 opportunities for methodological advances in fields including paleomagnetism, sediment  
697 provenance analysis, and seismology to overcome this impasse, unlocking the 60-25/13  
698 Ma interval of Tibetan and Himalayan evolution as natural laboratory for typical



699 geological responses for a-typical post-collisional subduction, or for a-typical geological  
700 responses to typical oceanic subduction.

701

## 702 Acknowledgements

703 I thank my friends and collaborators Wim Spakman, Pete Lippert, Carl Guilmette,  
704 Wentao Huang, Shihu Li, Zhenyu Li, Guillaume Dupont-Nivet, Abdul Qayyum, Paul  
705 Kapp, Thomas Schouten, Licheng Cao, and Eldert Advokaat for the many discussions  
706 that inspired me to write this paper.

707

## 708 Funding

709 This work was supported by Netherlands Organization for Scientific Research Vici grant  
710 865.17.001.

711

## 712 Author contributions

713 DJJvH is the sole author of this paper, performed analyses, and drafted figures.

714

715 **Figure captions**

716

717 **Fig. 1.** Reconstructed India-Asia convergence (21), which, when corrected for Tibetan  
718 shortening (11) predicts Indian plate subduction/underthrusting for the last 60 Ma. The  
719 amount of post-collisional subduction is a function of initial collision age recorded in the  
720 Himalaya (60-55 Ma) (18, 19, 45) and the width of horizontally underthrust India, which  
721 varies along-strike from 400-800 km (at the longitude of the reference location, this width  
722 is ~400 km, Fig. 2).

723

724 **Fig. 2.** Seismic tomographic images taken from the UU-P07 tomography model (50, 99).  
725 **A)** Vertical section from the Indian Ocean to Central Asia (drawn using the Hades  
726 Underworld Explorer, [www.atlas-of-the-underworld.org](http://www.atlas-of-the-underworld.org)). Deep, flat-lying slabs relate to  
727 Mesozoic Paleotethys and Mesotethys subduction during the amalgamation of Tibetan  
728 terranes (16). The India slab contains the bulk of Neotethys lithosphere that subducted  
729 northward below the Lhasa terrane, whereas the northward subducted but overturned  
730 Himalaya slab contains subducted Greater Indian lithosphere (11, 13, 16, 38, 39).  
731 Horizontally underthrust Indian continental lithosphere protrudes northward from the  
732 Main Frontal Thrust over a distance of 400-800 km, varying along-strike (9-12, 16). **B).**  
733 Horizontal cross-section at 110 km depth through the UU-P07 tomography model,  
734 overlain by outlines of modern geology and geography. The yellow dotted line depicts  
735 the outline of the northern margin of horizontally underthrust Indian continent below  
736 Tibet, protruding ~800 km northward north of the Himalayan syntaxes, decreasing to  
737 ~400 km towards ~90°E (9, 11, 12)

738

739 **Fig. 3.** Reconstructions of the diachronous onset of horizontal Indian underthrusting at  
740 **(A)** 25 Ma; **(B)** 13 Ma, and **(C)** the Present Day, using the outline of horizontally  
741 underthrust continental lithosphere of India shown in Figure tomography, using the

742 kinematic reconstruction of Tibet and the Himalaya of reference (11), and India-Asia  
743 convergence following reference (21).

744

745 **Fig. 4.** Paleogeographic maps at the time of initial collision (~60 Ma (18, 19, 45)) and in  
746 Gondwana fits at 155, corresponding to the timing of continental breakup in the Argo  
747 Abyssal Plain between Northwest Australia and the conceptual Argoland continent (51),  
748 for three end-member models discussed in the text. Models are placed in the  
749 paleomagnetic reference frame of reference (100). **A)** Model C, with a fully continental  
750 Greater India (19, 23, 24, 40); **B)** Model A, in which initial collision occurred with an  
751 intra-oceanic subduction zone around the equator. The size of continental Greater India is  
752 here constructed with a 40 Ma closure age of the remaining oceanic lithosphere (8, 25-28,  
753 52); Model C), in which 60 Ma collision occurs between a microcontinent that broke off  
754 Northern India in the Cretaceous, opening a Greater India Basin in its wake (11, 29).  
755 AAP = Argo Abyssal Plain; KLA = Kohistan-Ladakh Arc; PAO = Pakistan Ophiolites;  
756 TH = Tibetan Himalaya; WBB = West Burma Block; WFZ = Wallaby Fracture Zone;  
757 XFB = Xigaze Forearc Basin.

758

759 **Fig. 5.** Tectonic map of the India-Asia collision zone, modified after reference (11). Mct  
760 = Main Central Thrust; mft = Main Frontal Thrust; RRF = Red River Fault; std = South  
761 Tibetan Detachment.

762

763 **Fig. 6. A)** Tectonic map of the Himalaya and Tibet, simplified after references (58, 85,  
764 86). **B)** Schematic cross section through the Himalayas and southern Tibet, modified  
765 from reference (8). ATF = Altyn Tagh Fault; GCT = Great Counter Thrust; GT =  
766 Gangdese Thrust; IYSZ = Indus-Yarlung Suture Zone; KF = Karakoram Fault; MCT =  
767 Main Central Thrust; MFT = Main Frontal Thrust; MHT = Main Himalayan Thrust; STD  
768 = South Tibetan Detachment.

769

770 **Fig. 7.** Conceptual evolution of Himalayan architecture if **A)** all Eocene-early Miocene  
771 India-Asia convergence is accommodated to the north of the Himalaya. In this case, the  
772 MCT can have formed when the GH rocks decoupled from their original Indian lower  
773 crustal and lithospheric underpinnings, or **B)**, all or part of the Eocene-early Miocene  
774 India-Asia convergence is accommodated within the Himalaya. In this case, the MCT is  
775 an out-of-sequence thrust that formed within the early Miocene Himalayan fold-thrust  
776 belt and Eocene-Miocene units that may have accreted below the Greater Himalaya have  
777 been removed by subduction erosion.

778

779 **Fig. 8.** Cartoon illustrating geometrical relationships between diachronous slab  
780 detachment and onset of horizontal Indian continental lithospheric underthrusting below  
781 Tibet between 25 and 13 Ma, and geological expressions in the Tibetan Plateau.

782

783    **References**

784

785

786    1.     Vlaar, N, Wortel, M. Lithospheric aging, instability and subduction.  
787    *Tectonophysics*. 1976; **32**(3-4): 331-51.

788    2.     Cloos, M. Lithospheric buoyancy and collisional orogenesis: Subduction of  
789    oceanic plateaus, continental margins, island arcs, spreading ridges, and seamounts.  
790    *Geological Society of America Bulletin*. 1993; **105**(6): 715-37.

791    3.     Molnar, P, England, P, Martinod, J. Mantle dynamics, uplift of the Tibetan  
792    Plateau, and the Indian monsoon. *Reviews of Geophysics*. 1993; **31**(4): 357-96.

793    4.     Su, T, Spicer, RA, Li, S-H, *et al*. Uplift, climate and biotic changes at the  
794    Eocene–Oligocene transition in south-eastern Tibet. *National Science Review*. 2019; **6**(3):  
795    495-504.

796    5.     Xia, L, Li, X, Ma, Z, *et al*. Cenozoic volcanism and tectonic evolution of the  
797    Tibetan plateau. *Gondwana Research*. 2011; **19**(4): 850-66.

798    6.     Sun, X, Lu, Y, Li, Q, *et al*. A downgoing Indian lithosphere control on along-  
799    strike variability of porphyry mineralization in the Gangdese belt of southern Tibet.  
800    *Economic Geology*. 2021; **116**(1): 29-46.

801    7.     Nomade, S, Renne, PR, Mo, X, *et al*. Miocene volcanism in the Lhasa block,  
802    Tibet: spatial trends and geodynamic implications. *Earth and Planetary Science Letters*.  
803    2004; **221**(1-4): 227-43.

804    8.     Kapp, P, DeCelles, PG. Mesozoic–Cenozoic geological evolution of the  
805    Himalayan–Tibetan orogen and working tectonic hypotheses. *American Journal of*  
806    *Science*. 2019; **319**(3): 159-254.

807    9.     Li, J, Song, X. Tearing of Indian mantle lithosphere from high-resolution seismic  
808    images and its implications for lithosphere coupling in southern Tibet. *Proceedings of the*  
809    *National Academy of Sciences*. 2018; **115**(33): 8296-300.

810    10.    Chen, M, Niu, F, Tromp, J, *et al*. Lithospheric foundering and underthrusting  
811    imaged beneath Tibet. *Nature communications*. 2017; **8**(1): 1-10.

812    11.    van Hinsbergen, DJJ, Lippert, PC, Li, S, *et al*. Reconstructing Greater India:  
813    Paleogeographic, kinematic, and geodynamic perspectives. *Tectonophysics*. 2019; **760**:  
814    69-94.

815    12.    Agius, MR, Lebedev, S. Tibetan and Indian lithospheres in the upper mantle  
816    beneath Tibet: Evidence from broadband surface-wave dispersion. *Geochemistry,*  
817    *Geophysics, Geosystems*. 2013; **14**(10): 4260-81.

818    13.    Replumaz, A, Negredo, AM, Villaseñor, A, *et al*. Indian continental subduction  
819    and slab break-off during Tertiary collision. *Terra Nova*. 2010; **22**: 290-6.

820    14.    Nabelek, J, Hetenyi, G, Vergne, J, *et al*. Underplating in the Himalaya–Tibet  
821    collision zone revealed by the Hi-CLIMB experiment. *Science*. 2009; **325**(5946): 1371-4.

822    15.    Styron, R, Taylor, M, Sundell, K. Accelerated extension of Tibet linked to the  
823    northward underthrusting of Indian crust. *Nature Geoscience*. 2015; **8**(2): 131-4.

824    16.    Qayyum, A, Lom, N, Advokaat, EL, *et al*. Subduction and slab detachment under  
825    moving trenches during ongoing India–Asia convergence. *Earth and Space Science Open*  
826    *Archive*. 2022: 45.

- 827 17. Webb, AAG, Guo, H, Clift, PD, *et al.* The Himalaya in 3D: Slab dynamics  
828 controlled mountain building and monsoon intensification. *Lithosphere*. 2017.
- 829 18. An, W, Hu, X, Garzanti, E, *et al.* New precise dating of the India-Asia collision in  
830 the Tibetan Himalaya at 61 Ma. *Geophysical Research Letters*. 2021; **48**(3):  
831 e2020GL090641.
- 832 19. Hu, X, Garzanti, E, Wang, J, *et al.* The timing of India-Asia collision onset –  
833 Facts, theories, controversies. *Earth-Science Reviews*. 2016; **160**: 264-99.
- 834 20. van Hinsbergen, DJJ, Steinberger, B, Doubrovine, PV, *et al.* Acceleration and  
835 deceleration of India-Asia convergence since the Cretaceous: Roles of mantle plumes and  
836 continental collision. *Journal of Geophysical Research*. 2011; **116**(B6).
- 837 21. DeMets, C, Merkouriev, S. Detailed reconstructions of India–Somalia Plate  
838 motion, 60 Ma to present: implications for Somalia Plate absolute motion and India–  
839 Eurasia Plate motion. *Geophysical Journal International*. 2021; **227**(3): 1730-67.
- 840 22. van Hunen, J, Allen, MB. Continental collision and slab break-off: A comparison  
841 of 3-D numerical models with observations. *Earth and Planetary Science Letters*. 2011;  
842 **302**(1-2): 27-37.
- 843 23. Searle, MP. Timing of subduction initiation, arc formation, ophiolite obduction  
844 and India–Asia collision in the Himalaya. *Geological Society, London, Special  
845 Publications*. 2018; **483**: SP483. 8.
- 846 24. Ingalls, M, Rowley, DB, Currie, B, *et al.* Large-scale subduction of continental  
847 crust implied by India–Asia mass-balance calculation. *Nature Geoscience*. 2016; **9**(11):  
848 848-53.
- 849 25. Tapponnier, P, Mattauer, M, Proust, F, *et al.* Mesozoic ophiolites, sutures, and  
850 large-scale tectonic movements in Afghanistan. *Earth and Planetary Science Letters*.  
851 1981; **52**(2): 355-71.
- 852 26. Aitchison, JC, Ali, JR, Davis, AM. When and where did India and Asia collide?  
853 *Journal of Geophysical Research*. 2007; **112**(B5).
- 854 27. Martin, CR, Jagoutz, O, Upadhyay, R, *et al.* Paleocene latitude of the Kohistan–  
855 Ladakh arc indicates multistage India–Eurasia collision. *Proceedings of the National  
856 Academy of Sciences*. 2020; **117**(47): 29487-94.
- 857 28. Jagoutz, O, Royden, L, Holt, AF, *et al.* Anomalously fast convergence of India  
858 and Eurasia caused by double subduction. *Nature Geoscience*. 2015; **8**(6): 475-8.
- 859 29. van Hinsbergen, DJJ, Lippert, PC, Dupont-Nivet, G, *et al.* Greater India Basin  
860 hypothesis and a two-stage Cenozoic collision between India and Asia. *Proc Natl Acad  
861 Sci U S A*. 2012; **109**(20): 7659-64.
- 862 30. Cawood, PA, Kröner, A, Collins, WJ, *et al.* Accretionary orogens through Earth  
863 history. *Geological Society, London, Special Publications*. 2009; **318**(1): 1-36.
- 864 31. van Hinsbergen, DJJ, Schouten, TLA. Deciphering paleogeography from orogenic  
865 architecture: constructing orogens in a future supercontinent as thought experiment.  
866 *American Journal of Science*. 2021; **321**: 955-1031.
- 867 32. Borneman, NL, Hodges, KV, Van Soest, MC, *et al.* Age and structure of the  
868 Shyok suture in the Ladakh region of northwestern India: implications for slip on the  
869 Karakoram fault system. *Tectonics*. 2015; **34**(10): 2011-33.
- 870 33. Ding, L, Qasim, M, Jadoon, IAK, *et al.* The India–Asia collision in north  
871 Pakistan: Insight from the U–Pb detrital zircon provenance of Cenozoic foreland basin.  
872 *Earth and Planetary Science Letters*. 2016; **455**: 49-61.

- 873 34. Rowley, DB. Comparing Paleomagnetic Study Means with Apparent Wander  
874 Paths: A Case Study and Paleomagnetic Test of the Greater India versus Greater Indian  
875 Basin Hypotheses. *Tectonics*. 2019; **38**: 722-40.
- 876 35. Yuan, J, Yang, Z, Deng, C, *et al.* Rapid drift of the Tethyan Himalaya terrane  
877 before two-stage India-Asia collision. *National Science Review*. 2021; **8**(7): nwaal73.
- 878 36. Jadoon, UF, Huang, B, Shah, SA, *et al.* Multi-stage India-Asia collision:  
879 Paleomagnetic constraints from Hazara-Kashmir syntaxis in the western Himalaya. *GSA*  
880 *Bulletin*. 2021.
- 881 37. Yang, T, Jin, J, Bian, W, *et al.* Precollisional latitude of the Northern Tethyan  
882 Himalaya from the Paleocene redbeds and its implication for greater India and the India-  
883 Asia collision. *Journal of Geophysical Research: Solid Earth*. 2019; **124**(11): 10777-98.
- 884 38. Parsons, AJ, Hosseini, K, Palin, R, *et al.* Geological, geophysical and plate  
885 kinematic constraints for models of the India-Asia collision and the post-Triassic central  
886 Tethys oceans. *Earth-Science Reviews*. 2020: 103084.
- 887 39. Van der Voo, R, Spakman, W, Bijwaard, H. Tethyan subducted slabs under India.  
888 *Earth and Planetary Science Letters*. 1999; **171**(1): 7-20.
- 889 40. Replumaz, A, Tapponnier, P. Reconstruction of the deformed collision zone  
890 Between India and Asia by backward motion of lithospheric blocks. *Journal of*  
891 *Geophysical Research: Solid Earth*. 2003; **108**(B6).
- 892 41. van Hinsbergen, DJJ, Kapp, P, Dupont-Nivet, G, *et al.* Restoration of Cenozoic  
893 deformation in Asia and the size of Greater India. *Tectonics*. 2011; **30**(5): n/a-n/a.
- 894 42. Long, S, McQuarrie, N, Tobgay, T, *et al.* Geometry and crustal shortening of the  
895 Himalayan fold-thrust belt, eastern and central Bhutan. *Geological Society of America*  
896 *Bulletin*. 2011; **123**(7-8): 1427-47.
- 897 43. Patriat, P, Achache, J. India-Eurasia collision chronology has implications for  
898 crustal shortening and driving mechanism of plates. *Nature*. 1984; **311**: 615-21.
- 899 44. Hu, X, Garzanti, E, Moore, T, *et al.* Direct stratigraphic dating of India-Asia  
900 collision onset at the Selandian (middle Paleocene,  $59 \pm 1$  Ma). *Geology*. 2015; **43**(10):  
901 859-62.
- 902 45. Guillot, S, Mahéo, G, de Sigoyer, J, *et al.* Tethyan and Indian subduction viewed  
903 from the Himalayan high- to ultrahigh-pressure metamorphic rocks. *Tectonophysics*.  
904 2008; **451**(1-4): 225-41.
- 905 46. McKenzie, D, Priestley, K. The influence of lithospheric thickness variations on  
906 continental evolution. *Lithos*. 2008; **102**(1-2): 1-11.
- 907 47. England, P, Houseman, G. Extension during continental convergence, with  
908 application to the Tibetan Plateau. *Journal of Geophysical Research: Solid Earth*. 1989;  
909 **94**(B12): 17561-79.
- 910 48. Replumaz, A, Guillot, S, Villaseñor, A, *et al.* Amount of Asian lithospheric  
911 mantle subducted during the India/Asia collision. *Gondwana Research*. 2013; **24**(3-4):  
912 936-45.
- 913 49. Feng, J, Yao, H, Chen, L, *et al.* Massive lithospheric delamination in southeastern  
914 Tibet facilitating continental extrusion. *National Science Review*. 2021.
- 915 50. van der Meer, DG, van Hinsbergen, DJJ, Spakman, W. Atlas of the underworld:  
916 Slab remnants in the mantle, their sinking history, and a new outlook on lower mantle  
917 viscosity. *Tectonophysics*. 2018; **723**: 309-448.

- 918 51. Gibbons, AD, Barckhausen, U, van den Bogaard, P, *et al.* Constraining the  
919 Jurassic extent of Greater India: Tectonic evolution of the West Australian margin.  
920 *Geochemistry Geophysics Geosystems*. 2012; **13**.
- 921 52. Westerweel, J, Roperch, P, Licht, A, *et al.* Burma Terrane part of the Trans-  
922 Tethyan arc during collision with India according to palaeomagnetic data. *Nature*  
923 *Geoscience*. 2019; **12**(10): 863-8.
- 924 53. Isozaki, Y, Maruyama, S, Furuoka, F. Accreted oceanic materials in Japan.  
925 *Tectonophysics*. 1990; **181**(1-4): 179-205.
- 926 54. Agard, P, Yamato, P, Soret, M, *et al.* Plate interface rheological switches during  
927 subduction infancy: Control on slab penetration and metamorphic sole formation. *Earth*  
928 *and Planetary Science Letters*. 2016; **451**: 208-20.
- 929 55. van Hinsbergen, DJJ, Torsvik, T, Schmid, SM, *et al.* Orogenic architecture of the  
930 Mediterranean region and kinematic reconstruction of its tectonic evolution since the  
931 Triassic. *Gondwana Research*. 2020; **81**: 79-229.
- 932 56. Ziabrev, SV, Aitchison, JC, Abrajevitch, AV, *et al.* Bainang Terrane, Yarlung–  
933 Tsangpo suture, southern Tibet (Xizang, China): a record of intra-Neotethyan  
934 subduction–accretion processes preserved on the roof of the world. *Journal of the*  
935 *Geological Society*. 2004; **161**(3): 523-39.
- 936 57. An, W, Hu, X, Garzanti, E. Discovery of Upper Cretaceous Neo-Tethyan trench  
937 deposits in south Tibet (Luogangcuo Formation). *Lithosphere*. 2018; **10**(3): 446-59.
- 938 58. Guilmette, C, Hébert, R, Wang, C, *et al.* Geochemistry and geochronology of the  
939 metamorphic sole underlying the Xigaze Ophiolite, Yarlung Zangbo Suture Zone, South  
940 Tibet. *Lithos*. 2009; **112**(1-2): 149-62.
- 941 59. Garzanti, E. Stratigraphy and sedimentary history of the Nepal Tethys Himalaya  
942 passive margin. *Journal of Asian Earth Sciences*. 1999; **17**(5-6): 805-27.
- 943 60. DeCelles, PG, Kapp, P, Gehrels, GE, *et al.* Paleocene-Eocene foreland basin  
944 evolution in the Himalaya of southern Tibet and Nepal: Implications for the age of initial  
945 India-Asia collision. *Tectonics*. 2014; **33**(5): 824-49.
- 946 61. Carosi, R, Montomoli, C, Iaccarino, S. 20 years of geological mapping of the  
947 metamorphic core across Central and Eastern Himalayas. *Earth-Science Reviews*. 2018;  
948 **177**: 124-38.
- 949 62. Hodges, KV. Tectonics of the Himalaya and southern Tibet from two  
950 perspectives. *Geological Society of America Bulletin*. 2000; **112**(3): 324-50.
- 951 63. Yin, A. Cenozoic tectonic evolution of the Himalayan orogen as constrained by  
952 along-strike variation of structural geometry, exhumation history, and foreland  
953 sedimentation. *Earth-Science Reviews*. 2006; **76**(1-2): 1-131.
- 954 64. Smit, MA, Hacker, BR, Lee, J. Tibetan garnet records early Eocene initiation of  
955 thickening in the Himalaya. *Geology*. 2014; **42**(7): 591-4.
- 956 65. Grujic, D, Casey, M, Davidson, C, *et al.* Ductile extrusion of the Higher  
957 Himalayan Crystalline in Bhutan: evidence from quartz microfabrics. *Tectonophysics*.  
958 1996; **260**(1-3): 21-43.
- 959 66. Khan, I, Clyde, W. Lower Paleogene Tectonostratigraphy of Balochistan:  
960 Evidence for Time-Transgressive Late Paleocene-Early Eocene Uplift. *Geosciences*.  
961 2013; **3**(4): 466-501.



- 962 67. Qasim, M, Ahmad, J, Ding, L, *et al.* Integrated provenance and tectonic  
963 implications of the Cretaceous–Palaeocene clastic sequence, Changla Gali, Lesser  
964 Himalaya, Pakistan. *Geological Journal*. 2021; **56**(9): 4747-59.
- 965 68. Gaina, C, van Hinsbergen, DJJ, Spakman, W. Tectonic interactions between India  
966 and Arabia since the Jurassic reconstructed from marine geophysics, ophiolite geology,  
967 and seismic tomography. *Tectonics*. 2015; **34**(5): 875-906.
- 968 69. Gnos, E, Khan, M, Mahmood, K, *et al.* Bela oceanic lithosphere assemblage and  
969 its relation to the Reunion hotspot. *Terra Nova*. 1998; **10**(2): 90-5.
- 970 70. Robinson, DM, DeCelles, PG, Copeland, P. Tectonic evolution of the Himalayan  
971 thrust belt in western Nepal: Implications for channel flow models. *Geological Society of  
972 America Bulletin*. 2006; **118**(7-8): 865-85.
- 973 71. Beaumont, C, Jamieson, RA, Nguyen, M, *et al.* Himalayan tectonics explained by  
974 extrusion of a low-viscosity crustal channel coupled to focused surface denudation.  
975 *Nature*. 2001; **414**(6865): 738-42.
- 976 72. Jagoutz, O, Bouilhol, P, Schaltegger, U, *et al.* The isotopic evolution of the  
977 Kohistan Ladakh arc from subduction initiation to continent arc collision. *Geological  
978 Society, London, Special Publications*. 2019; **483**(1): 165-82.
- 979 73. Orme, DA. Burial and exhumation history of the Xigaze forearc basin, Yarlung  
980 suture zone, Tibet. *Geoscience Frontiers*. 2019; **10**(3): 895-908.
- 981 74. Einsele, G, Liu, B, Dürr, S, *et al.* The Xigaze forearc basin: evolution and facies  
982 architecture (Cretaceous, Tibet). *Sedimentary Geology*. 1994; **90**(1-2): 1-32.
- 983 75. Huang, W, van Hinsbergen, DJJ, Maffione, M, *et al.* Lower Cretaceous Xigaze  
984 ophiolites formed in the Gangdese forearc: Evidence from paleomagnetism, sediment  
985 provenance, and stratigraphy. *Earth and Planetary Science Letters*. 2015; **415**: 142-53.
- 986 76. Yin, A, Harrison, TM, Ryerson, F, *et al.* Tertiary structural evolution of the  
987 Gangdese thrust system, southeastern Tibet. *Journal of Geophysical Research: Solid  
988 Earth*. 1994; **99**(B9): 18175-201.
- 989 77. Maffione, M, van Hinsbergen, DJJ, Koornneef, LMT, *et al.* Forearc  
990 hyperextension dismembered the south Tibetan ophiolites. *Geology*. 2015; **43**(6): 475-8.
- 991 78. Li, Y, Li, R, Robinson, P, *et al.* Detachment faulting in the Xigaze ophiolite  
992 southern Tibet: New constraints on its origin and implications. *Gondwana Research*.  
993 2021; **94**: 44-55.
- 994 79. Yin, A, Harrison, TM. Geologic evolution of the Himalayan-Tibetan orogen.  
995 *Annual Review of Earth and Planetary Sciences*. 2000; **28**(1): 211-80.
- 996 80. Murphy, MA, Yin, A, Harrison, TM, *et al.* Did the Indo-Asian collision alone  
997 create the Tibetan plateau? *Geology*. 1997; **25**(8).
- 998 81. Li, S, van Hinsbergen, DJ, Najman, Y, *et al.* Does pulsed Tibetan deformation  
999 correlate with Indian plate motion changes? *Earth and Planetary Science Letters*. 2020;  
1000 **536**: 116144.
- 1001 82. Cowgill, E. Cenozoic right-slip faulting along the eastern margin of the Pamir  
1002 salient, northwestern China. *Geological Society of America Bulletin*. 2010; **122**(1-2):  
1003 145-61.
- 1004 83. Bullen, M, Burbank, D, Garver, J. Building the northern Tien Shan: Integrated  
1005 thermal, structural, and topographic constraints. *The Journal of Geology*. 2003; **111**(2):  
1006 149-65.

- 1007 84. Xiao, G, Guo, Z, Dupont-Nivet, G, *et al.* Evidence for northeastern Tibetan  
1008 Plateau uplift between 25 and 20 Ma in the sedimentary archive of the Xining Basin,  
1009 Northwestern China. *Earth and Planetary Science Letters*. 2012; **317**: 185-95.
- 1010 85. DeCelles, PG, Kapp, P, Quade, J, *et al.* Oligocene-Miocene Kailas basin,  
1011 southwestern Tibet: Record of postcollisional upper-plate extension in the Indus-Yarlung  
1012 suture zone. *Geological Society of America Bulletin*. 2011; **123**(7-8): 1337-62.
- 1013 86. Leary, R, Orme, DA, Laskowski, AK, *et al.* Along-strike diachroneity in  
1014 deposition of the Kailas Formation in central southern Tibet: Implications for Indian slab  
1015 dynamics. *Geosphere*. 2016; **12**(4): 1198-223.
- 1016 87. Li, S, Advokaat, EL, van Hinsbergen, DJJ, *et al.* Paleomagnetic constraints on the  
1017 Mesozoic-Cenozoic paleolatitudinal and rotational history of Indochina and South China:  
1018 Review and updated kinematic reconstruction. *Earth-Science Reviews*. 2017; **171**: 58-77.
- 1019 88. Bagheri, S, Gol, SD. The Eastern Iranian Orocline. *Earth-Science Reviews*. 2020:  
1020 103322.
- 1021 89. Coleman, M, Hodges, K. Evidence for Tibetan plateau uplift before 14 Myr ago  
1022 from a new minimum age for east–west extension. *Nature*. 1995; **374**(6517): 49-52.
- 1023 90. Gan, W, Molnar, P, Zhang, P, *et al.* Initiation of clockwise rotation and eastward  
1024 transport of southeastern Tibet inferred from deflected fault traces and GPS observations.  
1025 *GSA Bulletin*. 2021.
- 1026 91. Taylor, M, Yin, A. Active structures of the Himalayan-Tibetan orogen and their  
1027 relationships to earthquake distribution, contemporary strain field, and Cenozoic  
1028 volcanism. *Geosphere*. 2009; **5**(3): 199-214.
- 1029 92. Clark, MK, Royden, LH. Topographic ooze: Building the eastern margin of Tibet  
1030 by lower crustal flow. *Geology*. 2000; **28**(8).
- 1031 93. van Hinsbergen, DJJ, Spakman, W, de Boorder, H, *et al.* Arc-type magmatism  
1032 due to continental-edge plowing through ancient subduction-enriched mantle.  
1033 *Geophysical Research Letters*. 2020; **47**(9): e2020GL087484.
- 1034 94. Shen, T, Wang, G, Replumaz, A, *et al.* Miocene subsidence and surface uplift of  
1035 southernmost Tibet induced by Indian subduction dynamics. *Geochemistry, Geophysics,*  
1036 *Geosystems*. 2020; **21**(10): e2020GC009078.
- 1037 95. Capitanio, FA, Morra, G, Goes, S, *et al.* India–Asia convergence driven by the  
1038 subduction of the Greater Indian continent. *Nature Geoscience*. 2010; **3**(2): 136-9.
- 1039 96. Vaes, B, Gallo, LC, van Hinsbergen, DJ. On pole position: causes of dispersion of  
1040 the paleomagnetic poles behind apparent polar wander paths. *Earth and Space Science*  
1041 *Open Archive*. 2022; **preprint**.
- 1042 97. Saylor, JE, Sundell, KE. Quantifying comparison of large detrital geochronology  
1043 data sets. *Geosphere*. 2016; **12**(1): 203-20.
- 1044 98. Wei, SS, Shearer, PM, Lithgow-Bertelloni, C, *et al.* Oceanic plateau of the  
1045 Hawaiian mantle plume head subducted to the uppermost lower mantle. *Science*. 2020;  
1046 **370**(6519): 983-7.
- 1047 99. Amaru, M. *Global travel time tomography with 3-D reference models*: Utrecht  
1048 University; 2007.
- 1049 100. Torsvik, TH, Van der Voo, R, Preeden, U, *et al.* Phanerozoic polar wander,  
1050 palaeogeography and dynamics. *Earth-Science Reviews*. 2012; **114**(3-4): 325-68.

1051

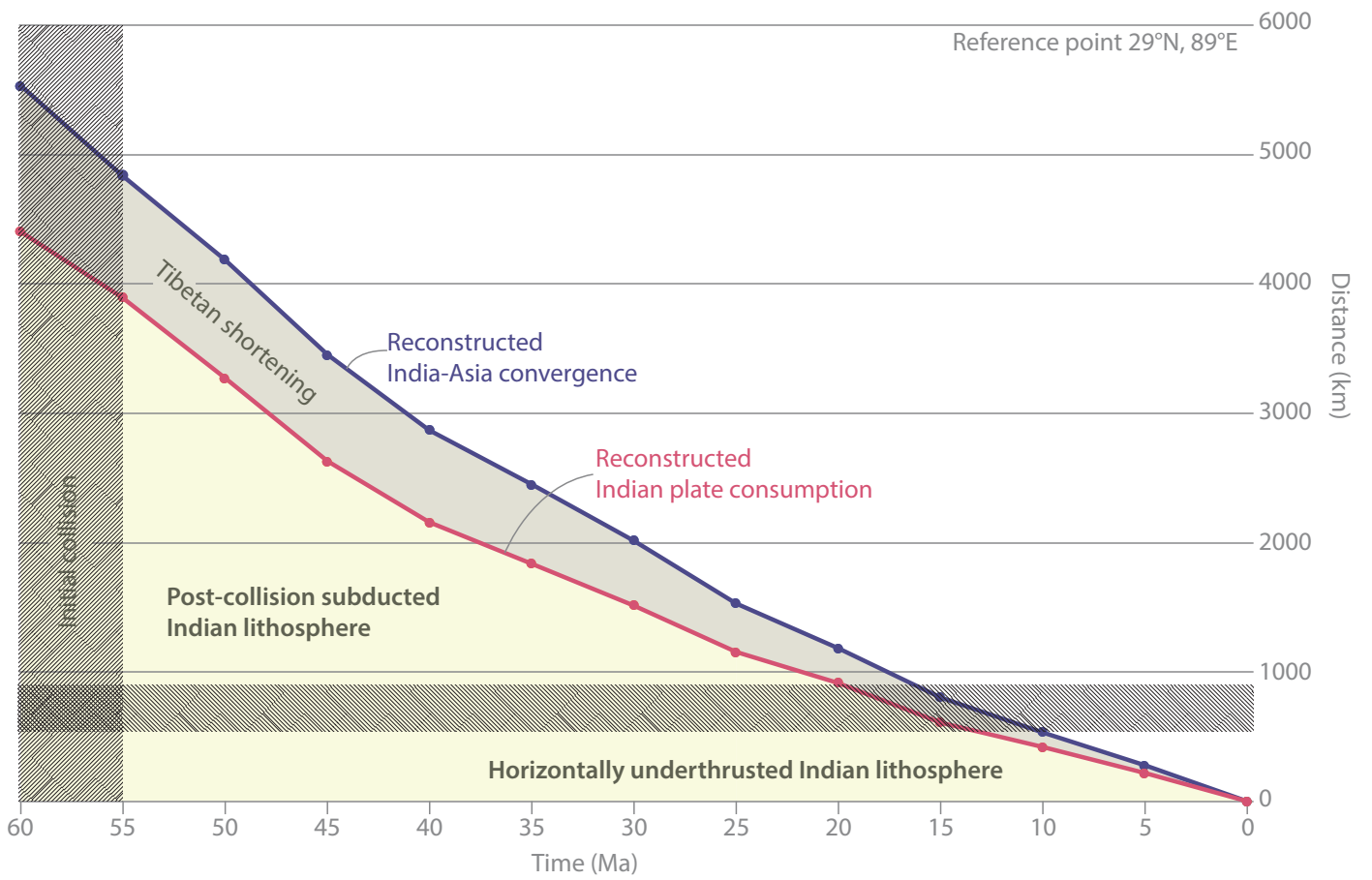


Figure 1

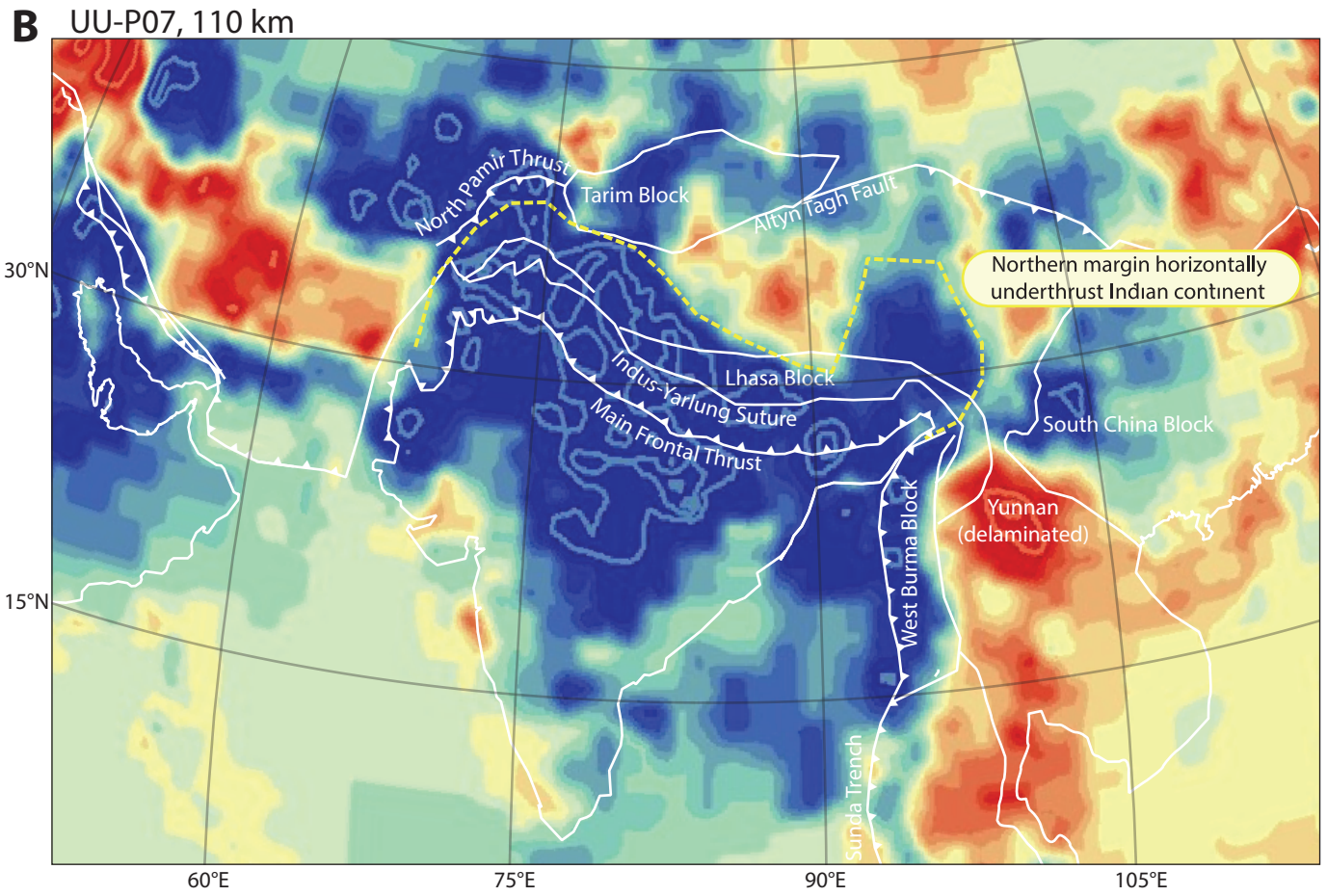
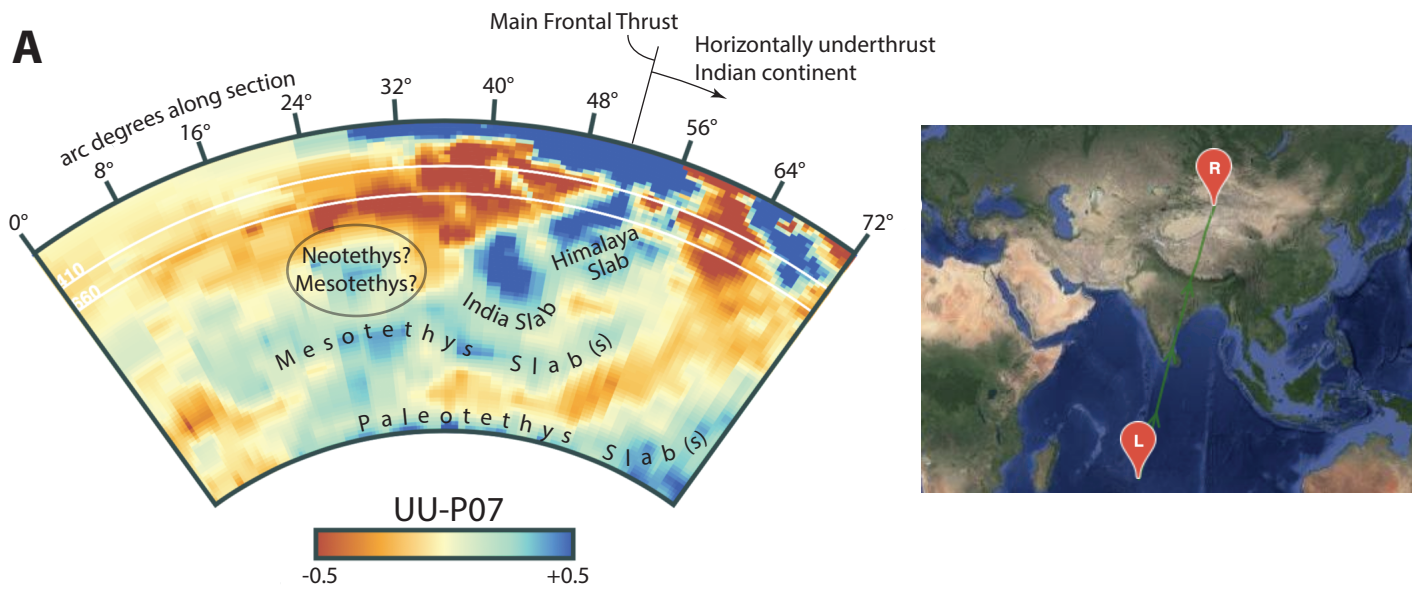


Figure 2

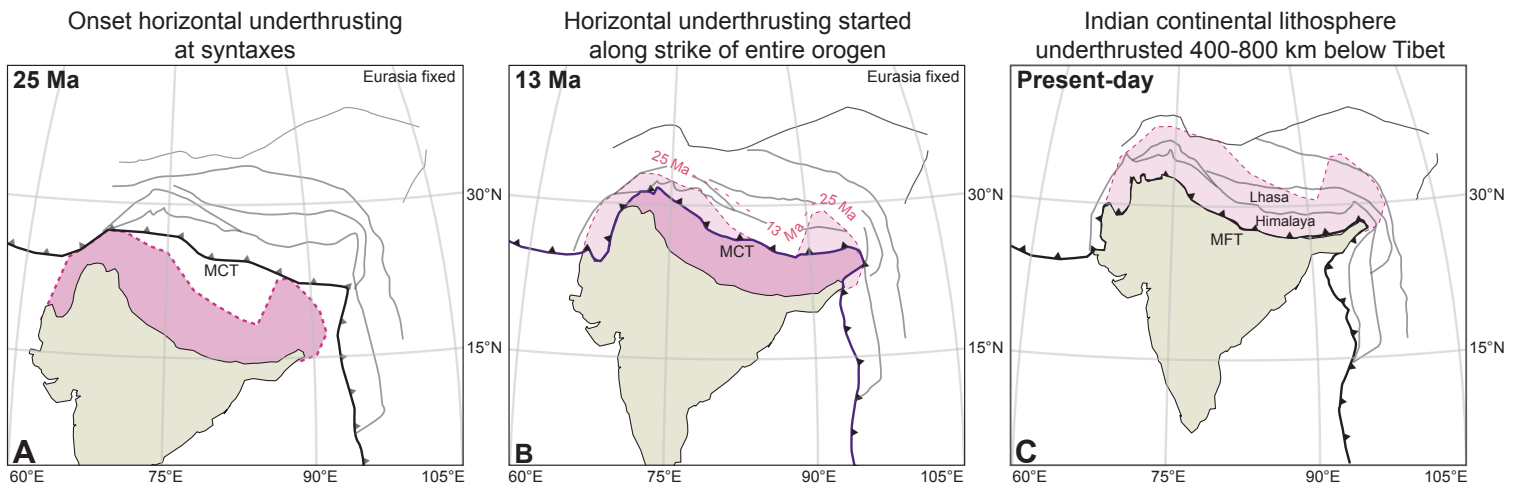


Figure 3

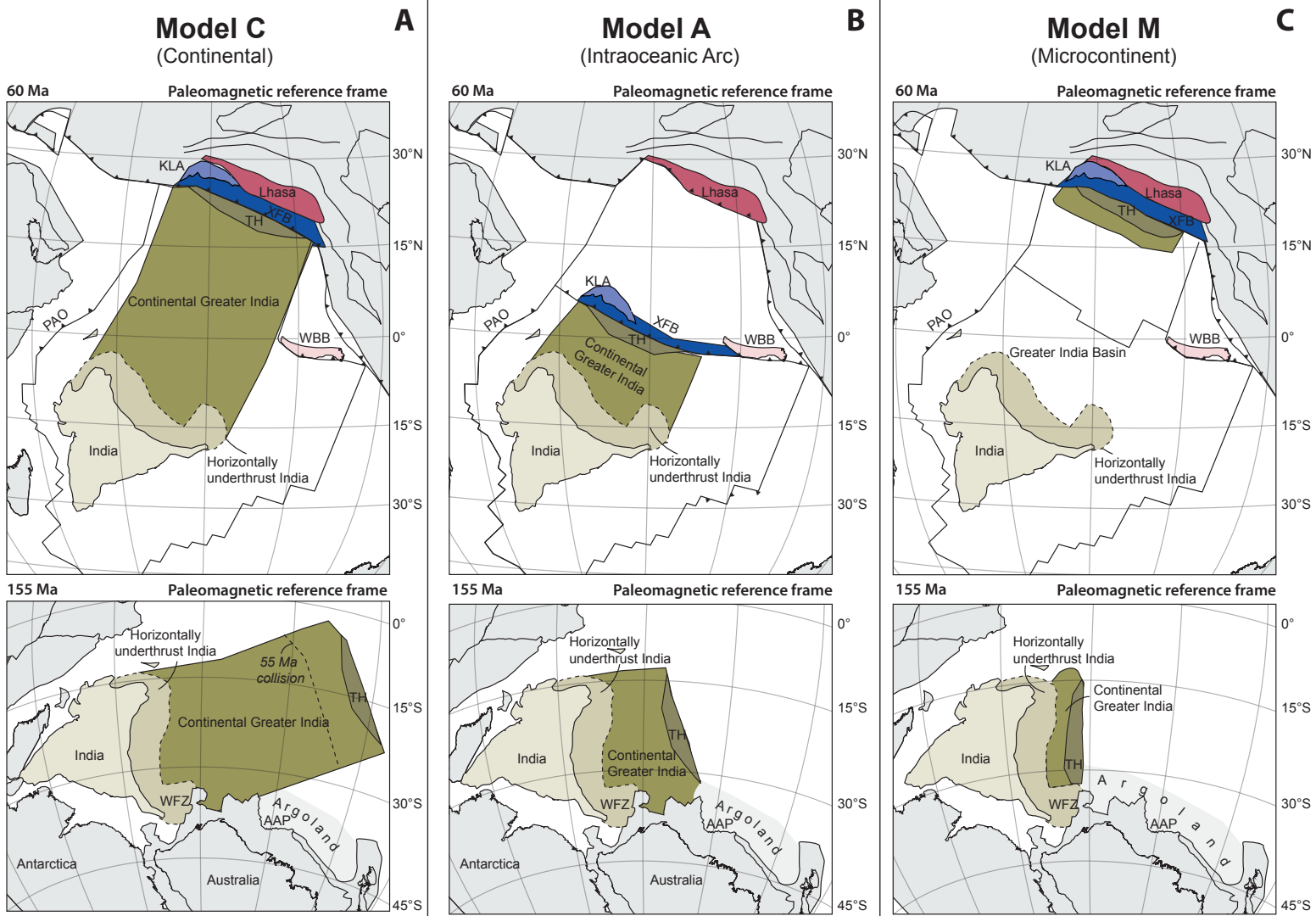


Figure 4

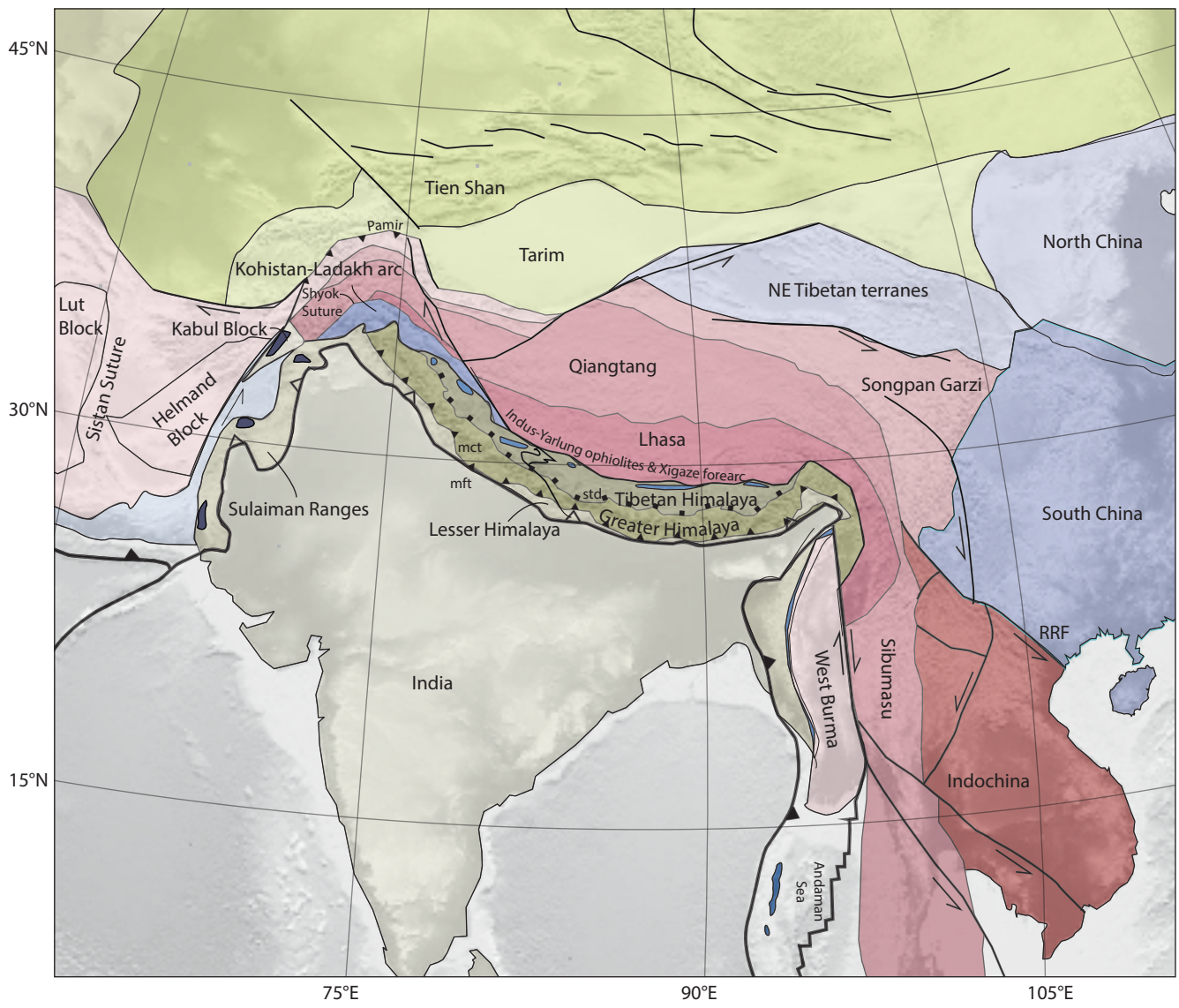


Figure 5

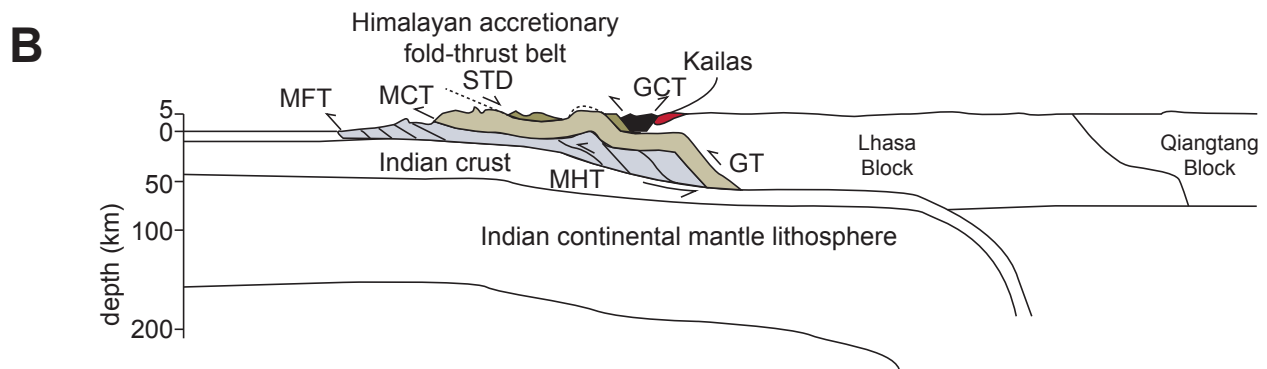
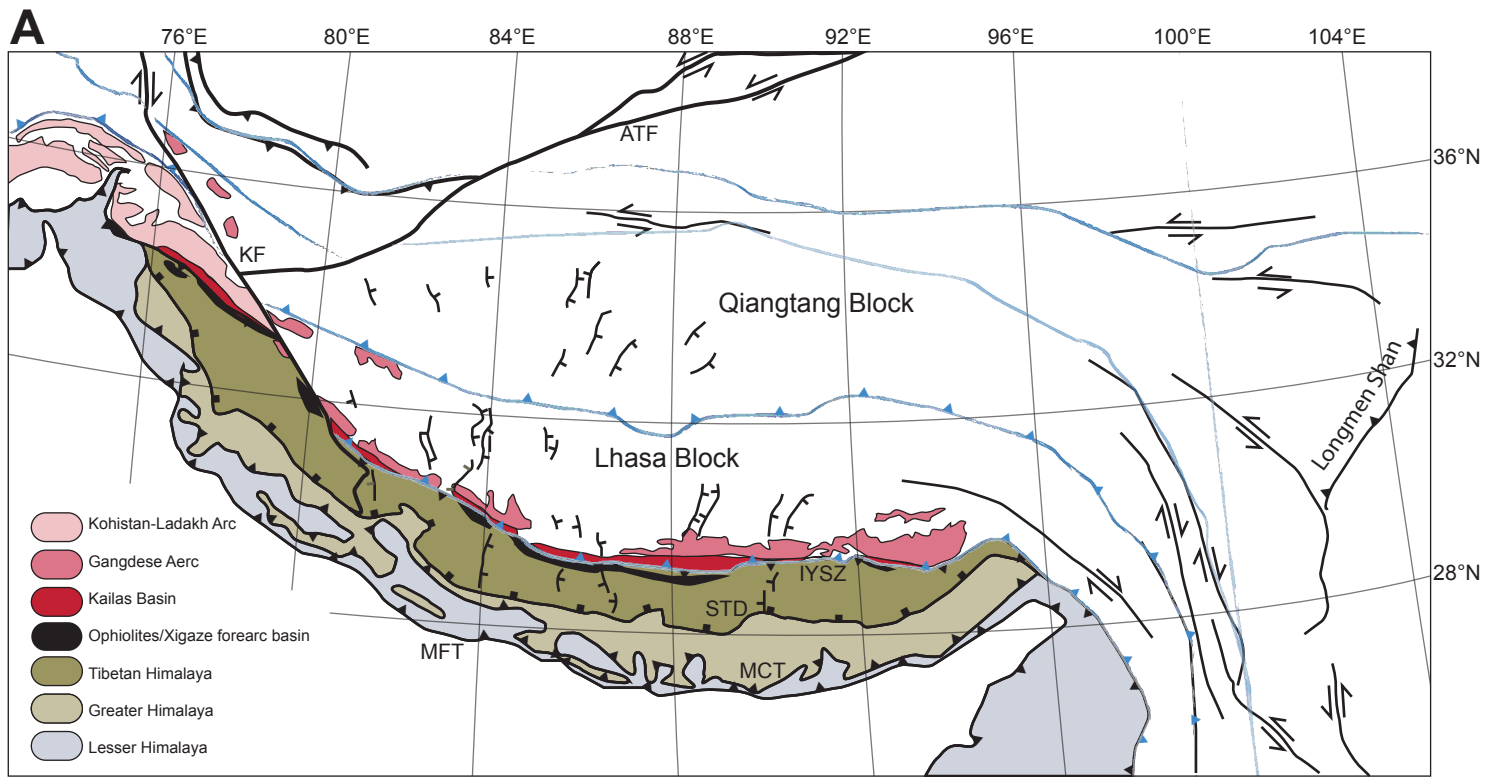
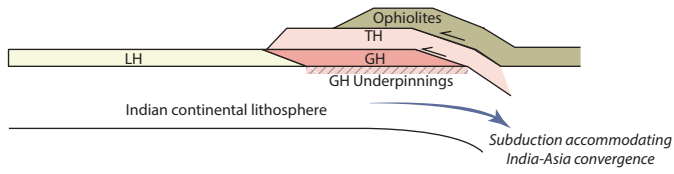


Figure 6

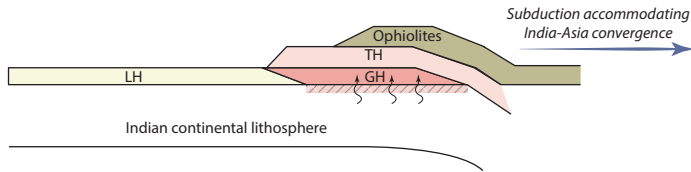


**A. Eocene-Miocene India-Asia convergence accommodated to the north of the Himalaya**

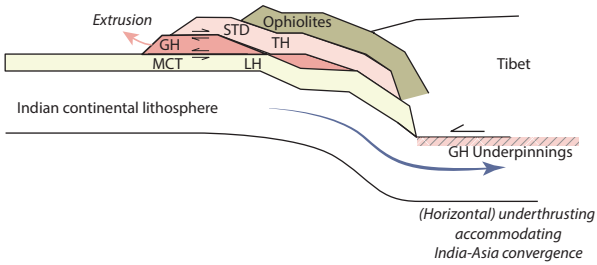
Late Paleocene-Early Eocene



Early Eocene-Early Miocene

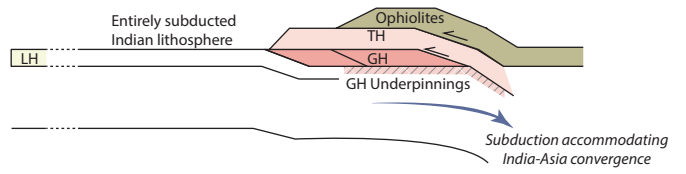


Early-Middle Miocene

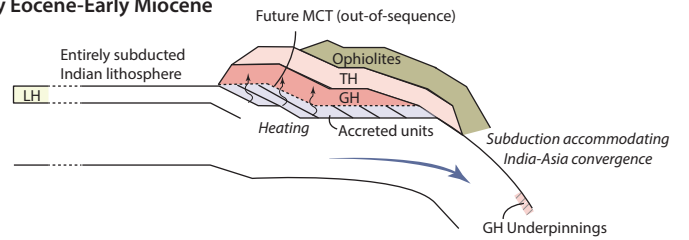


**B. Eocene-Miocene India-Asia convergence (partly) accommodated within the Himalaya**

Late Paleocene-Early Eocene



Early Eocene-Early Miocene



Early-Middle Miocene

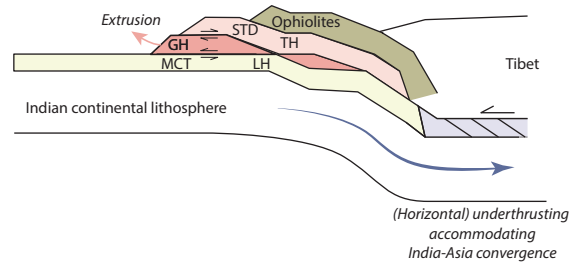


Figure 7

Miocene diachronous slab detachment and onset of horizontal underthrusting below Tibet

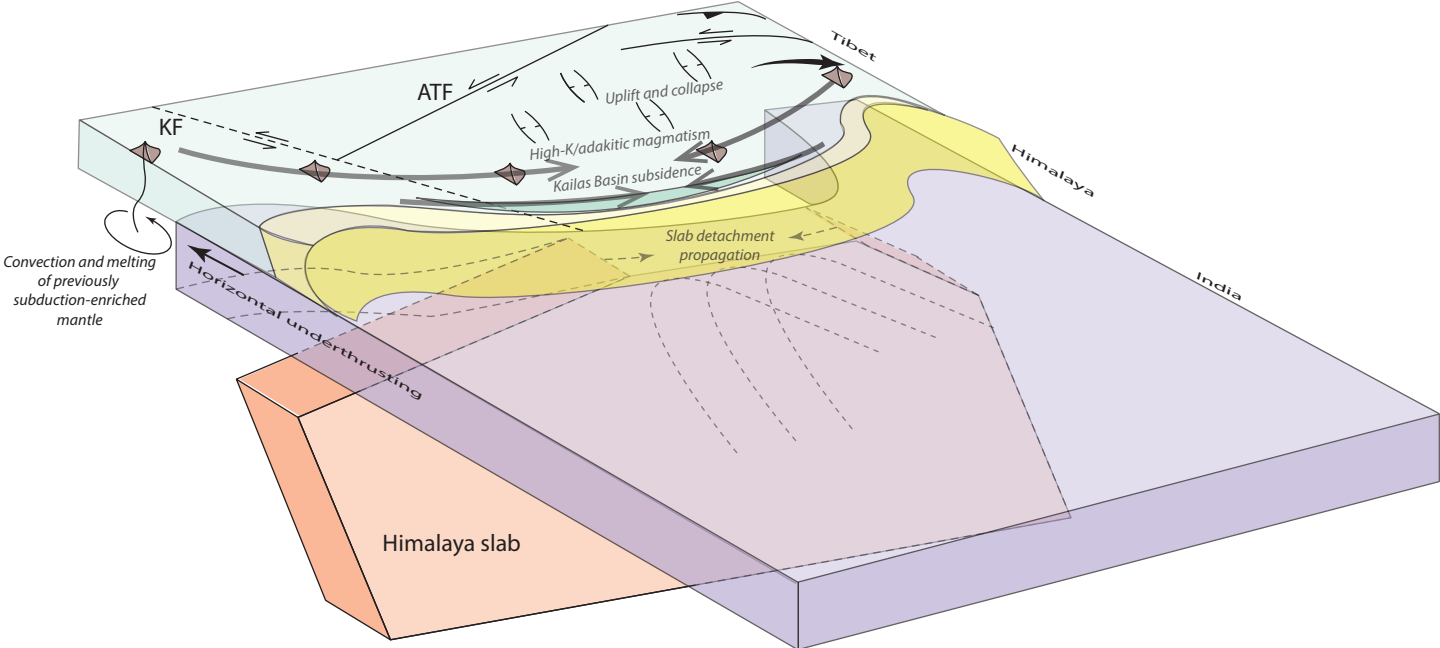


Figure 8